(This is a sample cover image for this issue. The actual cover is not yet available at this time.)

Global and Planetary Change 100 (2013) 51–69

Contents lists available at SciVerse ScienceDirect

Global and Planetary Change

journal homepage: www.elsevier.com/locate/gloplacha

The phase relation between atmospheric carbon dioxide and global temperature

Ole Humlum [a,b,*], Kjell Stordahl [c], Jan-Erik Solheim [d]

[a] Department of Geosciences, University of Oslo, P.O. Box 1047 Blindern, N-0316 Oslo, Norway
[b] Department of Geology, University Centre in Svalbard (UNIS), P.O. Box 156, N-9171 Longyearbyen, Svalbard, Norway
[c] Telenor Norway, Finance, N-1331 Fornebu, Norway
[d] Department of Physics and Technology, University of Tromsø, N-9037 Tromsø, Norway

ARTICLE INFO

Article history:
Received 25 April 2012
Accepted 25 August 2012
Available online 30 August 2012

Keywords:
Carbon dioxide
Global temperature
Sea surface temperature
Volcanic eruptions

ABSTRACT

Using data series on atmospheric carbon dioxide and global temperatures we investigate the phase relation (leads/lags) between these for the period January 1980 to December 2011. Ice cores show atmospheric CO_2 variations to lag behind atmospheric temperature changes on a century to millennium scale, but modern temperature is expected to lag changes in atmospheric CO_2, as the atmospheric temperature increase since about 1975 generally is assumed to be caused by the modern increase in CO_2. In our analysis we use eight well-known datasets: 1) globally averaged well-mixed marine boundary layer CO_2 data, 2) HadCRUT3 surface air temperature data, 3) GISS surface air temperature data, 4) NCDC surface air temperature data, 5) HadSST2 sea surface data, 6) UAH lower troposphere temperature data series, 7) CDIAC data on release of anthropogene CO_2, and 8) GWP data on volcanic eruptions. Annual cycles are present in all datasets except 7) and 8), and to remove the influence of these we analyze 12-month averaged data. We find a high degree of co-variation between all data series except 7) and 8), but with changes in CO_2 always lagging changes in temperature. The maximum positive correlation between CO_2 and temperature is found for CO_2 lagging 11–12 months in relation to global sea surface temperature, 9.5–10 months to global surface air temperature, and about 9 months to global lower troposphere temperature. The correlation between changes in ocean temperatures and atmospheric CO_2 is high, but do not explain all observed changes.

1. Introduction

Ice core records indicate that the greenhouse gas CO_2 co-varied with the global temperature over several glacial–interglacial cycles, suggesting a link between natural atmospheric greenhouse gas variations and temperature on long time scales (IPCC AR4, 2007; Lüthi et al., 2008).

Over the last 420 kyr variations in atmospheric CO_2 broadly followed temperature according to ice cores, with a typical delay of several centuries to more than a millennium (Lorius et al., 1990; Mudelsee, 2001; Caillon et al., 2003). Atmospheric CO_2 is therefore not initiating the large glacial–interglacial climate changes, and presumably these are controlled by orbital Milankovitch cycles. It has however been suggested that the subsequent CO_2-rise may amplify or even in certain periods precede the global temperature increase initiated by Milankovitch cycles, but the interpretation of the proxy data is ambiguous with regard to this (Alley and Clarck, 1999; Shackleton, 2000; Toggweiler and Lea, 2010; Shakun et al., 2012).

The observed time lag between atmospheric temperature and CO_2 from ice cores is thought to be caused by the slow vertical mixing that occurs in the oceans, in association with the decrease in the solubility of CO_2 in ocean water, as its temperature slowly increase at the end of glacial periods (Martin et al., 2005), leading to subsequent net out-gassing of CO_2 from the oceans (Toggweiler, 1999).

Direct measurements of temperatures and atmospheric CO_2 with good time resolution are essential to understand empirically the effects of CO_2 on modern global temperature changes. The first *in situ* continuous measurements of atmospheric CO_2 made by a high-precision non-dispersive infrared gas analyzer were implemented by C.D. Keeling from the Scripps Institution of Oceanography (SIO). These measurements were initiated in 1958 at Mauna Loa, Hawaii, located at 19°N in the Pacific Ocean (Keeling et al., 1995). These data documented that not only was the amount of CO_2 increasing in the atmosphere since 1958, but also that the rise was modulated by annual cycles caused by seasonal changes in ocean surface temperature and photosynthesis in the terrestrial biosphere.

The Mauna Loa measurements were followed by other continuous *in situ* measurements at a limited number of other observation sites in both hemispheres (Conway et al., 1994; Nakazawa et al., 1997; Langenfelds et al., 2002). In the 1980s and 1990s, however, it was recognized that a greater coverage of CO_2 measurements over continental areas was required to provide the basis for estimating sources and sinks of

* Corresponding author at: Department of Geosciences, University of Oslo, P.O. Box 1047 Blindern, N-0316 Oslo, Norway. Tel.: +47 41403157.
E-mail address: Ole.Humlum@geo.uio.no (O. Humlum).

0921-8181/$ – see front matter © 2012 Elsevier B.V. All rights reserved.
http://dx.doi.org/10.1016/j.gloplacha.2012.08.008

atmospheric CO_2 over land as well as ocean regions, and to provide basis for calculating a good estimate of the global amount of atmospheric CO_2.

2. Modern global CO_2 and temperature

Today, an extensive network of international air sampling sites is operated by the National Oceanic and Atmospheric Administration's Global Monitoring Division (NOAA/GMD) in the USA. This organization has measured carbon dioxide and other greenhouse gases for several decades at a globally distributed network of air sampling sites (Conway et al., 1994; IPCC AR4, 2007). A global average is constructed by fitting a smoothed curve as a function of time to each site, and then the smoothed value for each site is plotted as a function of latitude for 48 equal time steps per year (IPCC AR4, 2007). A global average is calculated from the latitude plot at each time step (Masarie and Tans, 1995), based on measurements from a subset of network sites. Only sites where samples are predominantly of well-mixed marine boundary layer (MBL) air representative of a large volume of the atmosphere are considered for the global CO_2 data series (IPCC AR4, 2007). These key sites are typically at remote marine sea level locations with prevailing onshore winds, to minimize the effects of inland vegetation and industries. Measurements from sites at higher altitude and from sites close to anthropogenic and natural sources and sinks are excluded from the global CO_2 estimate. The MBL data provide a low-noise representation of the global trend and allows making the estimate directly from the data without the need for applying an atmospheric transport model (IPCC AR4, 2007).

Global monthly CO_2 data (NOAA) are available from January 1980, and is shown graphically in Fig. 1, along with the monthly global sea surface temperature (HadSST2) and the monthly global surface air temperature (HadCRUT3), using data published by the University of East Anglia and the Hadley Centre, UK. In addition, in the present study we also analyze global air temperature data from the Goddard Institute for Space Studies (GISS) in USA, the National Climatic Data Center (NCDC) in USA, and lower troposphere temperature data published by the University of Alabama (UAH), Huntsville, USA. At the end of the paper a list of URL's used to obtain the data used can be found. All these monthly data series are now sufficiently long to have collected a population of climate perturbations, and they are therefore likely to reveal essentials of the coupling between atmospheric CO_2 and temperature in modern time.

Global atmospheric CO_2 (Fig. 1) has increased steadily during the entire observation period since 1980. There is, however, a pronounced annual cyclic variation superimposed on this overall development, caused by seasonal changes in the magnitude of sources and sinks for CO_2, controlled by dynamic exchanges with oceans and vegetation (IPCC AR4, 2007). The two temperature series HadSST2 and HadCRUT3 also show an overall increase over the period, but their detailed development is more complex than for CO_2. In addition, they only show small net changes since early 2002 (Scafetta, 2011).

In general, the two temperature records are seen to vary in close concert with each other. This also applies for the three other temperature records considered in this study (GISS, NCDC and UAH), but these are not displayed in Fig. 1 to avoid visual congestion. All four temperature records display rhythmic annual variations because of the uneven hemispherical distribution of land and ocean, although this is not readily apparent from the diagram, as other short-term variations tend to dominate.

Resolving the degree of coupling between CO_2 and temperature is not visually straightforward as illustrated by Fig. 1, but obviously requires a more elaborate approach to the data series.

3. DIFF12 values

Before analyzing the monthly data, being interested in longer than annual variations, we first removed the annual cycle from the global atmospheric CO_2 data series by calculating a 12-month running average. This implies that we here consider the annual variation as noise only, and instead are looking for the underlying longer signal, the overall CO_2 increase. As the signal tends to be almost the same from one monthly observation to nearby observations and the noise does not, an average of several adjacent monthly observations will tend to converge on the value of the signal alone. The most serious

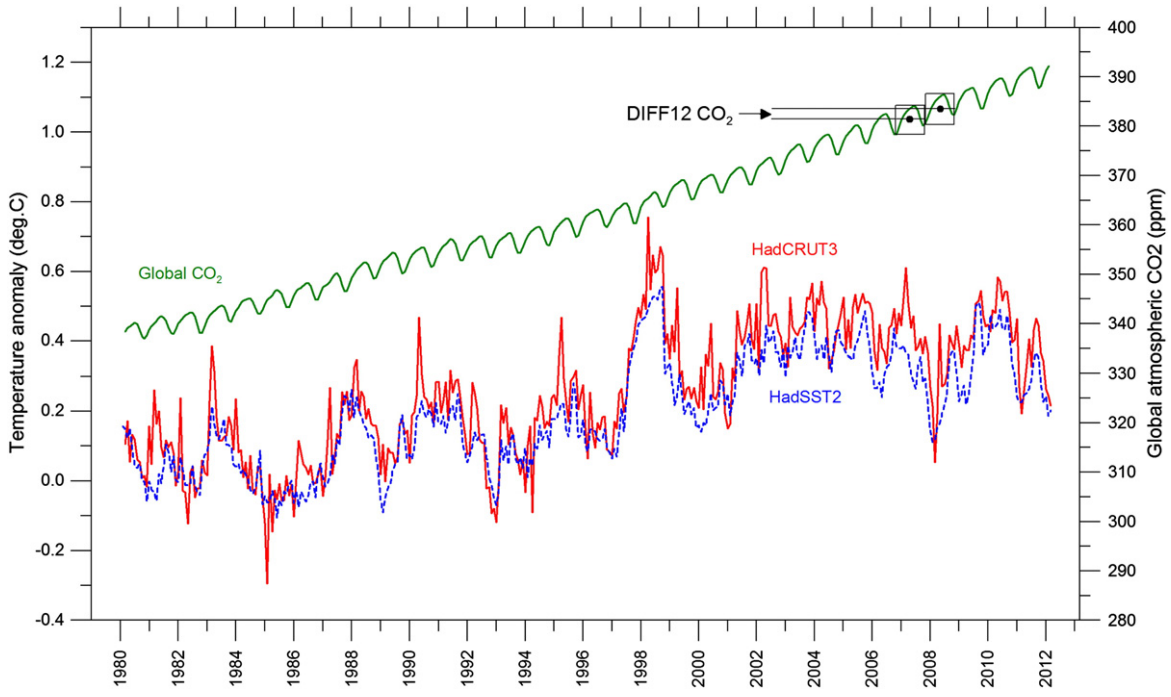

Fig. 1. Monthly global atmospheric CO_2 (NOOA; green), monthly global sea surface temperature (HadSST2; blue stippled) and monthly global surface air temperature (HadCRUT3; red), since January 1980. Last month shown is December 2011. (For interpretation of the references to color in this figure legend, the reader is referred to the web version of the article.)

consequence of smoothing or filtering is the shift of peaks and troughs in the smoothed curve, relative to the original data. If several data series are to be compared, identical filtering must therefore be applied at all series, as spurious effects else may arise, perhaps even inviting a false interpretation (see, e.g., discussion in Stauning, 2011).

We next calculated the difference between the average CO_2 concentration for the last 12 months and the average for the preceding 12 month period, referred to as DIFF12 in the following (see Fig. 1 for graphical explanation). In other words, DIFF 12 represents the yearly net change with monthly time resolution. Technically DIFF12 values were plotted for the last month considered in the calculation. By this we can efficiently visualize and analyze changes in the overall atmospheric CO_2 increase since January 1980, without confounding influence by the annual variation.

It is important to stress that the presence of a DIFF12 peak do not indicate the presence of a concentration peak in the original CO_2 data, but instead a period with more rapid increase than else. It is also worth emphasizing that by studying DIFF12 values we are investigating change rates in the amount of atmospheric CO_2, and not the total amount of CO_2 itself. However, by integrating DIFF12 values over the observation period, changes in the total amount of CO_2 are of cause addressed. Thus, to the degree that DIFF12 values can be explained, changes in the total amount of atmospheric CO_2 are therefore also explained.

We next compared the result of the DIFF12 CO_2 calculation with similar DIFF12 values for the global sea surface (HadSST2) and the global surface air temperature (HadCRUT3). By this all monthly data series were exposed to identical operations and the results are therefore comparable. To ensure that no spurious effects were introduced by the data filtering we carried out a similar analysis on the unfiltered monthly data, by calculating $DIFF1_{annual}$, defined as the difference between 1 month and the identical month 1 yr before, e.g. January 2000 minus January 1999, etc. Finally, all $DIFF1_{annual}$ and DIFF12 series were calculated and plotted in a time-change diagram (Fig. 2), to obtain graphical overview.

From Fig. 2 it is seen that the 12-month filtering process results in a displacement of DIFF12 peak and minimum values 12 months ahead in time in relation to the unfiltered $DIFF1_{annual}$ values, exactly as expected from definition of DIFF12. More important, however, it is also seen that the relation between peaks and lows in the different data series as to their relative timing remains unchanged. If no time displacement of peaks and lows by filtering was important for the following analysis, this might have been obtained simply by changing the plotting convention, and plotting DIFF12 at the last month in the first 12-month interval, instead of at the last month in the second interval. Thus, by using a 12-month filter as outlined above we acquire a considerably clearer picture of the underlying signal in the individual data series (Fig. 2), compared to the unfiltered data (Fig. 1).

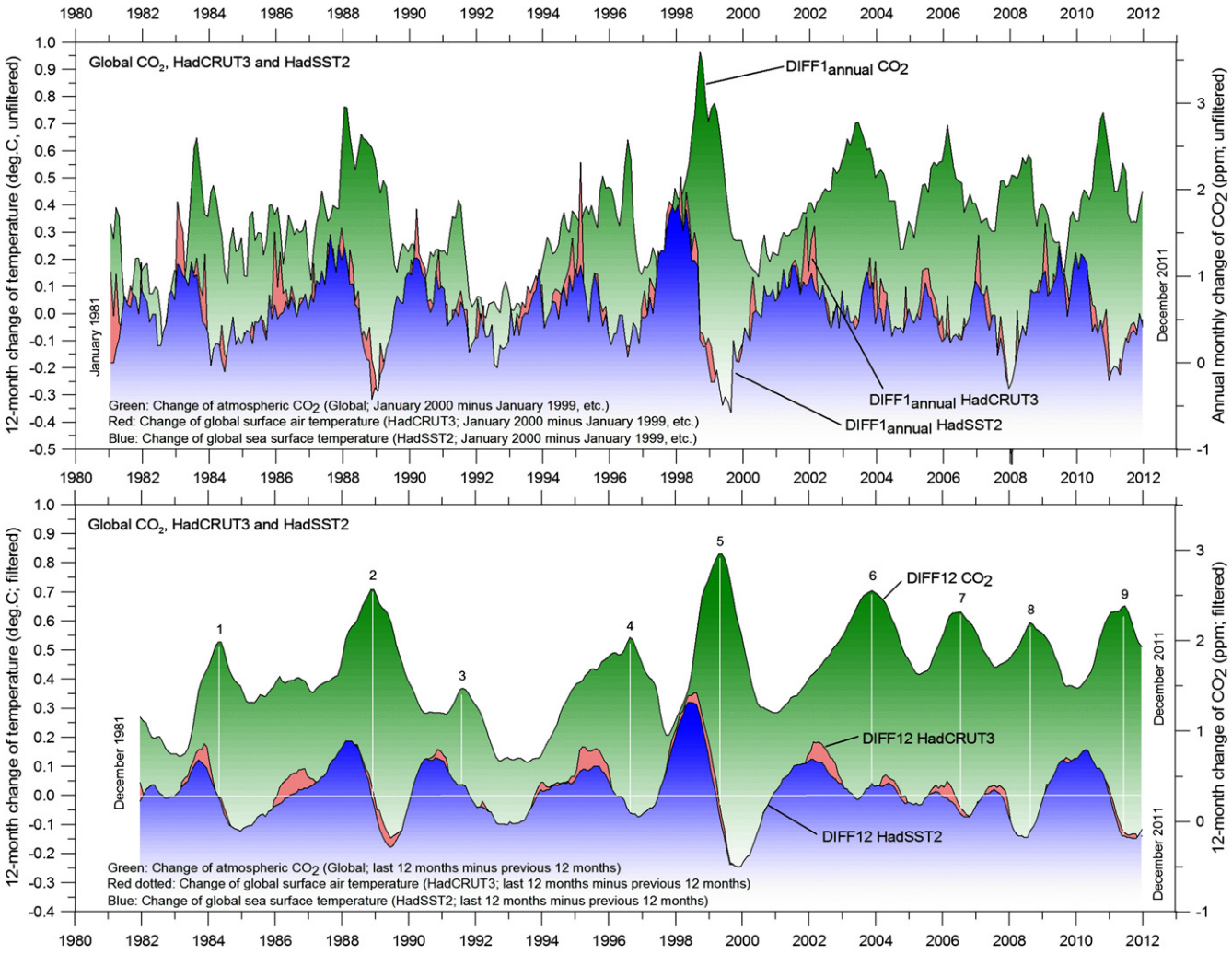

Fig. 2. 12-month change of global atmospheric CO_2 concentration (NOAA; green), global sea surface temperature (HadSST2; blue) and global surface air temperature (HadCRUT3; red dotted). The upper panel shows unfiltered monthly values (e.g. January 2000 minus January 1999), while the lower panel shows filtered values (DIFF12, the difference between the average of the last 12 month and the average for the previous 12 months for each data series). The numbers (1–9) on DIFF12 CO_2 peaks and the thin white lines refer to Table 1. (For interpretation of the references to color in this figure legend, the reader is referred to the web version of the article.)

The difference to Fig. 1 in vertical scale used for displaying DIFF12 values should be borne in mind when inspecting Fig. 2, especially for CO_2, but the visual impression is nevertheless instructive. The DIFF12 graph for CO_2 always remain positive, between 0.5 and 3 ppm per year, a consequence of the steady increase in atmospheric CO_2 over the observation period. The average DIFF12 is about 1.7 ppm/yr, which as expected adds up to the entire overall increase of 51 ppm in atmospheric CO_2 between 1980 and 2011. From about 2004, the average and minimum DIFF12 values for atmospheric CO_2 are somewhat higher than before, but the data series is too short to evaluate if this is a significant development or not.

The monthly development of DIFF12 for the two temperature records is more complicated, ranging from positive to negative values, reflecting repeated periods of warming and cooling over time windows of 12 months. However, the most conspicuous observation is that all three DIFF12-graphs display variations in concert with each other, suggesting internal coupling or, alternatively, the common effect of another factor, influencing all three variables.

Fig. 3 shows the result of an identical analysis, but here using global surface air temperature data from the Goddard Institute for Space Studies (GISS), USA. The general visual impression is identical to that conveyed by Fig. 2: all three DIFF12 graphs vary in close concert with each other.

4. DIFF12 surface temperature analyses

A detailed inspection of Figs. 2 and 3 provides some important clues to what appears to be an important relation between global temperature and atmospheric CO_2. For example, the prominent temperature change peak associated with the well-known 1998 El Niño event is seen to precede the corresponding CO_2 change peak by almost 1 yr, and similar lags of several months are seen for most of the other DIFF12 CO_2 peaks. There are nine main DIFF12 atmospheric CO_2 peaks visible in Fig. 2, and Table 1 show these nine peak values for DIFF12 CO_2 and the corresponding nine DIFF12 values for HadSST2 and HadCRUT3. From this it is seen that DIFF12 CO_2 peak values generally are associated with negative or near zero DIFF12 values for both HadSST2 and HadCRUT3.

One additional intriguing detail can be observed in both Figs. 2 and 3. The sea surface temperature change peaks typically occurs shortly before the corresponding global surface air temperature change peak, suggesting a characteristic sequence of events: 1) change of the global sea surface temperature, 2) change of global surface air temperature, and 3) change of global atmospheric CO_2 content. In other words, on this background global temperature changes appear to be initiated at the surface of the oceans.

Fig. 4 shows the correlation coefficient calculated for the DIFF12 surface temperature (GISS, HadCRUT3 and HadSST2) and global CO_2 data, to investigate the time lag of atmospheric CO_2 in relation to the three different surface temperature records. The maximum positive correlation between CO_2 and temperature is found for CO_2 lagging about 9.5 months after GISS, 10 months after HadCRUT3 and 11 months after HadSST2.

In other words, a change of atmospheric CO_2 typically follows about 11 months after the corresponding change of sea surface temperatures, and 9.5–10 months later than the global surface air temperature, again showing that changes in sea surface temperature typically occur a little (1–1.5 months) before corresponding changes in the global surface air temperature. The strongest positive correlation coefficient (0.45) between CO_2 and temperature is found towards the HadSST2 sea surface temperature. However, the difference to surface air temperatures is relatively small, and the maximum positive correlation coefficient is 0.40 for HadCRUT3 and 0.43 for GISS.

5. DIFF12 land and ocean temperature analysis

The NCDC data series on surface air temperatures makes it possible to analyze the phase relation between atmospheric CO_2 and subsets of surface air temperatures calculated for land, ocean, and global surface areas, respectively. To achieve this, all three NCDC datasets were exposed to the DIFF12 numerical procedure described above. The result is shown in Fig. 5.

The DIFF12 NCDC data for land areas show more marked variations than the corresponding ocean and global surface air temperature records. As expected, the ocean record is showing the smallest temperature change rates, reflecting the large difference in heat capacity between land and ocean surfaces. However, all three DIFF12 NCDC series are seen to vary in concert with each other, as well as with the DIFF12 CO_2 series. As was the case for the previously investigated temperature series, changes in the global atmospheric CO_2 data series are seen to lag behind corresponding changes in the NCDC temperatures.

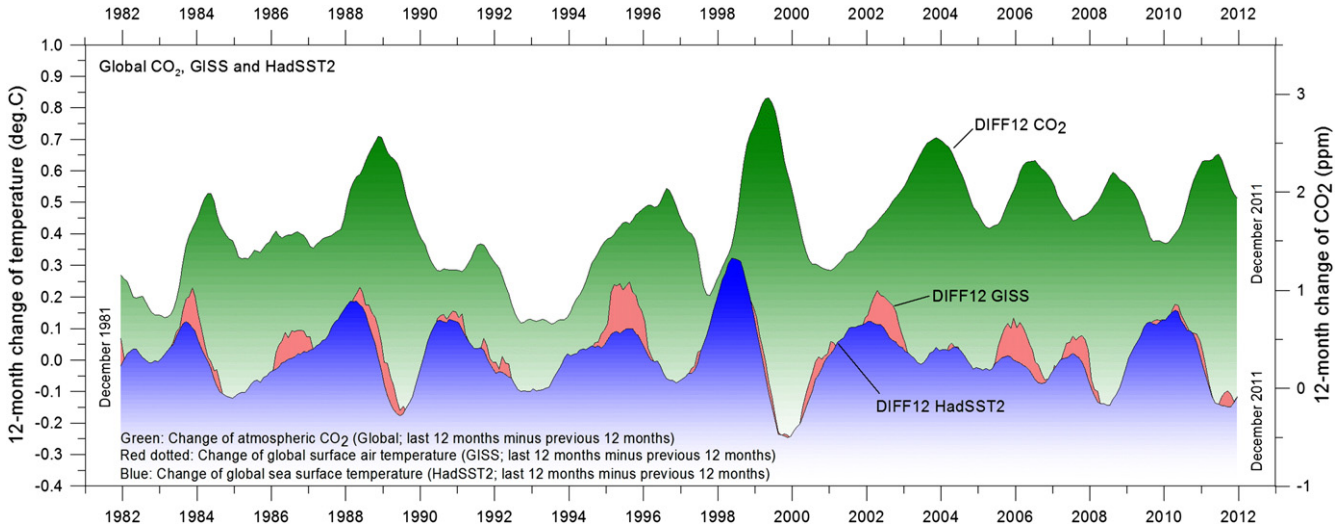

Fig. 3. 12-month change of global atmospheric CO_2 concentration (NOAA; green), global sea surface temperature (HadSST2; blue) and global surface air temperature (GISS; red dotted). All graphs are showing monthly values of DIFF12, the difference between the average of the last 12 months and the average for the previous 12 months for each data series. (For interpretation of the references to color in this figure legend, the reader is referred to the web version of the article.)

Table 1
Summary of peak DIFF12 CO_2 values and associated DIFF12 HadSST2 and HadCRUT3 values (Fig. 2). Underlining indicates negative values.

Peak DIFF12 CO_2	1	2	3	4	5	6	7	8	9
Value DIFF12 CO_2	1.984	2.570	1.472	2.037	2.958	2.552	2.322	2.201	2.383
Value DIFF12 HadSST2	−0.004	0.005	0.038	−0.059	−0.107	0.040	−0.063	−0.123	−0.127
Value DIFF12 HadCRUT3	−0.002	0.046	0.030	−0.098	−0.072	−0.005	−0.043	−0.150	−0.139

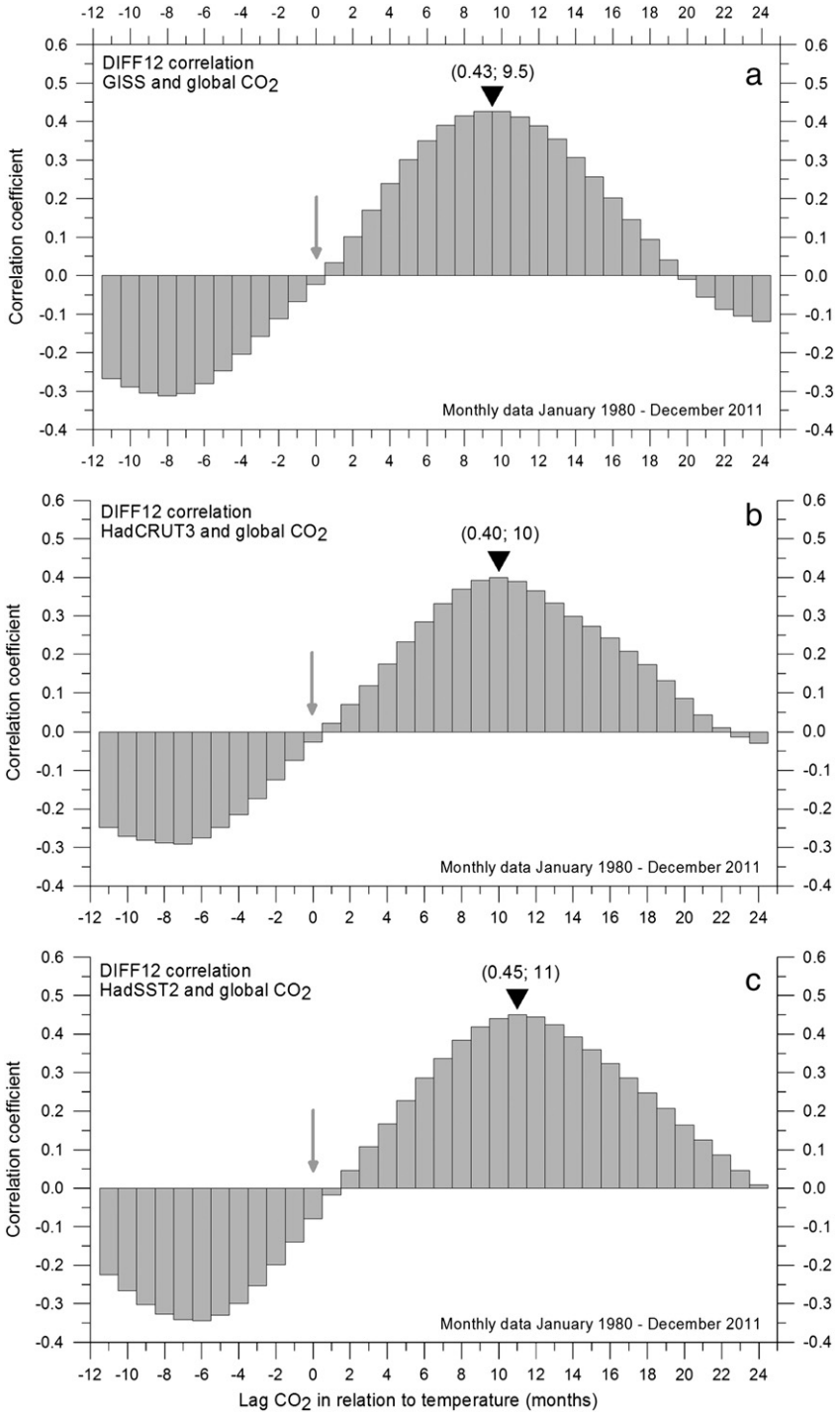

Fig. 4. Correlation coefficients between DIFF12 monthly surface air temperatures (a: GISS; b: HadCRUT3), sea surface temperature (c: HadSST2) and global atmospheric CO_2, for different monthly lags of CO_2. The maximum positive correlation is found for CO_2 lagging 9.5 months behind GISS, 10 months behind HadCRUT3 and 11 months behind HadSST2. Numbers in parentheses show the maximum positive correlation coefficient and the associated time lag of CO_2 in months. The grey vertical arrows indicate no lag.

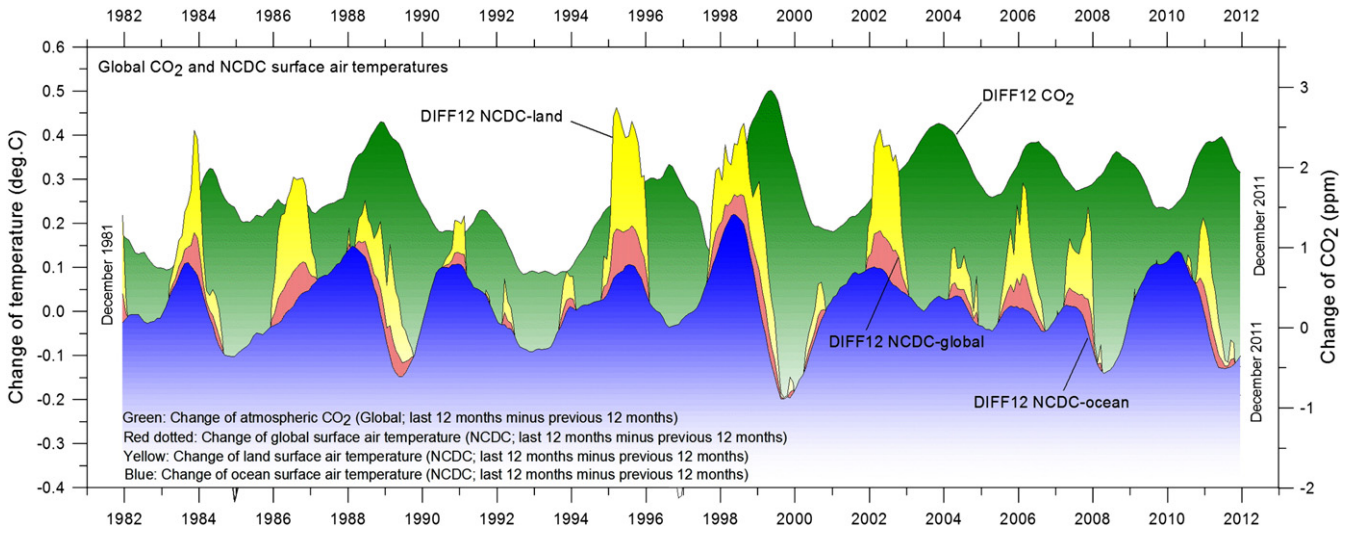

Fig. 5. 12-month change of global atmospheric CO_2 concentration (NOAA; green), change in global surface air temperature (NCDC; blue), land surface air temperature (NCDC; yellow) and ocean surface air temperature (NCDC; red dotted). All graphs are showing monthly values of DIFF12, the difference between the average of the last 12 months and the average for the previous 12 months for each data series. (For interpretation of the references to color in this figure legend, the reader is referred to the web version of the article.)

Fig. 6 shows statistics of the CO_2 lag in relation to the three different NCDC surface air temperature series, when seen over the entire study period. The maximum positive correlation (0.45) between temperature and CO_2 is found for changes in atmospheric CO_2 lagging 12 months behind ocean surface air temperature. The lag is shorter (9.5 months) in relation to land surface air temperature, with a maximum positive correlation coefficient of only 0.29. In relation to the global (land and ocean) NCDC temperature atmospheric CO_2 has a maximum positive correlation (0.39) for a lag of 10 months after corresponding changes in temperature.

Thus, summing up for the analysis of the NCDC data, changes in atmospheric CO_2 is lagging 9.5–12 months behind changes in surface air temperatures calculated for the two main types of planetary surface, land and ocean, respectively. The strongest correlation (0.45) between atmospheric CO_2 and NCDC temperature is found in relation to ocean surface air temperatures, suggesting a rather strong coupling from changes in ocean temperature to changes in atmospheric CO_2.

6. DIFF12 troposphere temperature analyses

The above observations all suggest the ocean surface temperature to be an initiating factor in a planetary sequence of events, coupling temperature and atmospheric CO_2. Therefore, maintaining a special focus on the oceans (covering about 71% of the planetary surface), we proceed to investigate the lag between the changes of temperatures in the lower troposphere above oceans only, compared to associated changes in global atmospheric CO_2. This is shown in Fig. 7, using A) data on global atmospheric CO_2 and B) data on lower troposphere temperatures above oceans (UAH). Here tropical oceans are defined as oceans within 20 degrees north and south of the Equator. To ensure that our analysis is comparable with the previous analysis, all four data series were exposed to the DIFF12 yearly change procedure described above.

In general, the DIFF12 temperature change peaks for these three important ocean regions are seen to be more or less simultaneous (Fig. 7), but with the lower troposphere temperature change above the Northern Oceans lagging slightly behind corresponding changes above the Southern and the Tropical Oceans. This suggests that ocean surface temperature changes generally are initiated in the Southern Hemisphere or near the Equator. However, notwithstanding these comparatively small internal lags in the ocean temperature changes as reflected in the lower troposphere, the corresponding peaks and lows in the DIFF12 change rate of atmospheric CO_2 are clearly lagging several months after the lower troposphere temperature change above all three main ocean regions.

Fig. 8 shows the correlation coefficient between DIFF12 for global atmospheric CO_2 and DIFF12 for lower troposphere temperature (UAH) over land, ocean and global, respectively, for different lags of CO_2 in relation to temperature. The time lag is 8 months for land areas, 10 months for oceans, and 9 months for both land and oceans. The time lag of CO_2 is slightly shorter (1 month) than found for the surface temperature records, but changes in atmospheric CO_2 clearly lag the associated changes in all three lower troposphere temperatures analyzed. The correlation coefficient for the global 9-month lag is 0.48.

The overall shorter time lag of CO_2 in relation to lower troposphere temperatures, compared to surface temperatures, suggests a typical sequence of temperature change events starting at the planet surface and propagating to the lower troposphere with about one month delay, given the time resolution of the data series.

7. DIFF12 hemispheric temperature analyses

The above observations suggest the ocean surface temperature to be an initiating factor in a planetary sequence of events, coupling temperature and atmospheric CO_2. This motivates an analysis of the relation between global atmospheric CO_2 and surface air temperature in the two hemispheres separately (Fig. 9), as especially the surface of the Southern Hemisphere is dominated by oceans, and the lower troposphere temperature change above the northern oceans appears to be lagging slightly behind corresponding changes above the southern and the tropical oceans.

Here we show hemispherical temperatures according to NCDC, but other temperature records (HadCRUT3 and GISS) show essential an identical picture. The visual impression gained from Fig. 9 is similar to what is shown by the analysis above: DIFF12 variations for atmospheric CO_2 are tracking behind both sets of hemispherical surface air temperatures. However, because of the dominance of oceans in the Southern Hemisphere, the temperature change rates are smaller here than in the Northern Hemisphere. An inspection of Fig. 9 reveals that each DIFF12 temperature peak for the Southern Hemisphere is followed by a corresponding DIFF12 peak in global atmospheric CO_2. Usually Northern Hemisphere DIFF12 peaks occur in concert with Southern Hemisphere peaks, but there are a few occasions where a Northern Hemisphere DIFF12 temperature peak occurs independently (e.g., early 1986), and

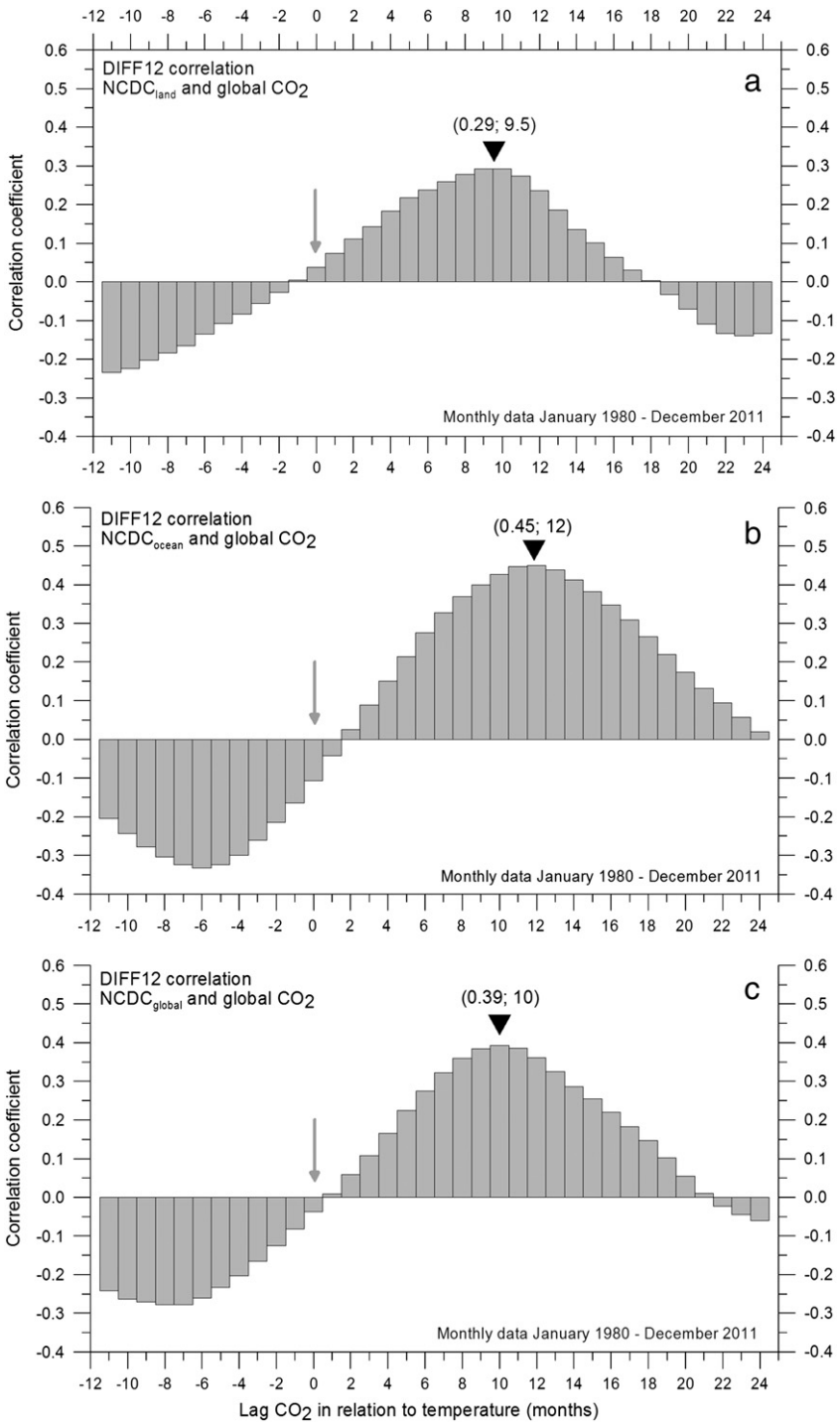

Fig. 6. Correlation coefficients between DIFF12 monthly NCDC surface air temperatures (a: land; b: ocean; c: global) and global atmospheric CO_2, for different monthly lags of CO_2. The maximum positive correlation is found for CO_2 lagging 9.5 months behind land surface air temperature, 12 months behind ocean surface air temperature and 10 months behind the global surface air temperature. Numbers in parentheses show the maximum positive correlation coefficient and the associated time lag of CO_2 in months. The grey vertical arrows indicate no lag.

is not followed by a corresponding DIFF12 CO_2 peak. By this the visual analysis thus favors a mainly Southern Hemisphere coupling to DIFF12 CO_2 peaks.

Fig. 10 shows the correlation coefficient between DIFF12 for global atmospheric CO_2 and DIFF12 for Northern and Southern Hemisphere temperature (NCDC), respectively, for different lags of CO_2 in relation to temperature. Positive correlation is found only for DIFF12 CO_2 lagging DIFF12 temperature. The maximum positive correlation is found for DIFF12 atmospheric CO_2 lagging about 9.5 months behind Northern Hemisphere temperature, and 11 months behind Southern Hemisphere temperature, suggesting the Southern Hemisphere to be leading the dynamics shown in Fig. 9. The correlation coefficient is considerably higher (0.56) for the Southern Hemisphere than for the Northern Hemisphere (0.26), indicating the association between changes in hemispherical temperature and changes in global atmospheric CO_2 to be especially strong for the Southern Hemisphere. Thus, both analyses suggest a mainly Southern Hemisphere origin of observed DIFF12 changes for atmospheric CO_2.

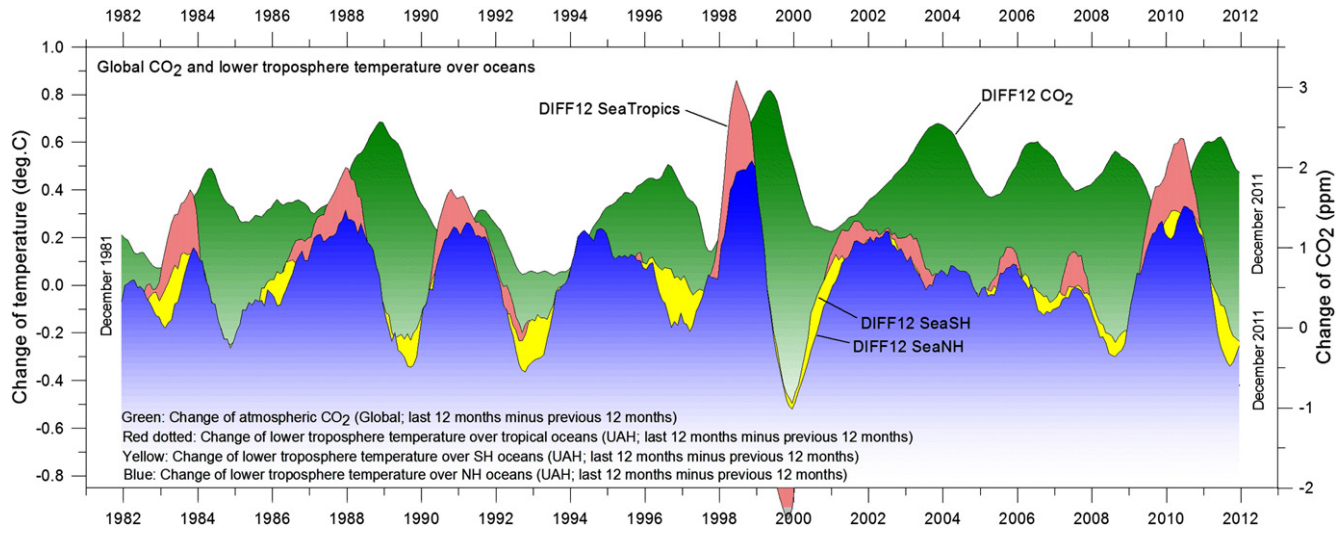

Fig. 7. 12-month change of global atmospheric CO_2 concentration (NOAA; green), change in lower troposphere temperature over oceans in the Northern Hemisphere (UAH; blue), in the Southern Hemisphere (UAH; yellow) and in the Tropics (UAH; red dotted). All graphs are showing monthly values of DIFF12, the difference between the average of the last 12 months and the average for the previous 12 months for each data series. (For interpretation of the references to color in this figure legend, the reader is referred to the web version of the article.)

8. DIFF12 release of CO_2 from anthropogene sources

We next investigated the degree of correlation between atmospheric CO_2 and the release of CO_2 from different anthropogene sources, using monthly data from the Carbon Dioxide Information Analysis Center (CDIAC). DIFF12 values were calculated as above, and the result is shown in Fig. 11. Since 2009 only annual data are at hand, and these were therefore extrapolated on a flat average monthly basis. The inclusion of these data in the present analysis is important, as the increase in atmospheric CO_2 since 1958 usually is ascribed to anthropogene release of CO_2 from anthropogene sources. It is generally assumed that about half of the emitted anthropogene CO_2 is absorbed by the oceans and on land by various physical and chemical processes, leaving about the remaining half to explain the rise in global atmospheric CO_2.

Fig. 11 shows visually that the coupling between DIFF12 changes in anthropogene CO_2 and DIFF12 changes in atmospheric CO_2 is weak, especially when compared to what was the case for temperatures (Figs. 2, 3, 5, 7 and 9). Several of the change rate peaks in anthropogene CO_2 appear to lag behind peaks in atmospheric CO_2. In other cases, the direction of change is opposed to each other, as is exemplified by the pronounced 1998 El Niño peak in atmospheric CO_2, corresponding to almost zero change in anthropogene CO_2. The 2011 change peak for atmospheric CO_2 is another example, as this occurs simultaneously with the negative change rate for anthropogene CO_2, caused by the recent economical crisis. A similar contrast has previously been pointed out (Jaworowski et al., 1992) for Mauna Loa CO_2 data during the petroleum crisis 1973–74.

As anthropogene CO_2 generally is assumed to explain the modern rise in atmospheric CO_2, DIFF12 for this is expected to lag somewhat after DIFF12 for anthropogene CO_2. In contrast to this, Fig. 11 appears to suggest the opposite relation, if anything. This might partly be due to the extraordinary high use of fossil fuels especially in the Northern Hemisphere for heating purposes in relatively cold periods, which associates with DIFF12 CO_2 lows (Fig. 2). However, a detailed analysis of this falls beyond the present investigation.

In general the coupling appears visually weak compared to the previous comparisons with temperature (Figs. 2, 3, 5, 7 and 9). The relation between the two CO_2 data series also appears partly conflicting, and is difficult to determine precisely on a visual basis alone. However, it is evident from the visual analysis that changes in atmospheric CO_2 are generally not tracking changes in anthropogene emissions, which is contrary to expectation, if anthropogene CO_2 is the main driver for the observed rise in global atmospheric CO_2.

The release of CO_2 from fossil fuels into the atmosphere is strongly asymmetrical, with the overwhelming majority being released in the Northern Hemisphere around 40°N (Fig. 12). This motivates a hemispherical analysis of the relation between changes in anthropogene CO_2 released and changes in atmospheric CO_2. Due to the asymmetrical release pattern the influence of anthropogene CO_2 would be expected to be stronger and more direct in the Northern Hemisphere, compared to the Southern Hemisphere.

Fig. 13 shows the relation between DIFF12 for anthropogene CO_2 and DIFF12 values for atmospheric CO_2 recorded at four different stations representing a transect from the High Arctic to the South Pole. Here we are using the period from July 1991 to December 2006, as data (NOAA) only are available from all four stations for this time window. Once again, there is no direct visual coupling from the DIFF12 values for anthropogene CO_2 to any of the four individual records, but instead the DIFF12 values for anthropogene CO_2 appears to lag somewhat after DIFF12 values for all individual records.

Comparing the dynamic behavior of the four DIFF12 series for atmospheric CO_2, a systematic sequence however stands out: peaks and lows in DIFF12 values for Ascension Island (8°S) tend to occur shortly before the DIFF12 values for Mauna Loa (20°N), which leads before the DIFF12 values for the South Pole (90°S), which leads before the DIFF12 values for Alert (82°N) in the High Arctic. From this, changes in atmospheric CO_2 appear to be initiated near or a short distance south of the Equator, and from there spread towards the two poles within a year or so. En route, the signal presumable is modulated by local and regional effects, as is indicated by the much larger annual CO_2 variation (not shown here) in the High Arctic, compared to that recorded at the South Pole. There is however no indications of the main signal originating at mid-latitudes in the Northern Hemisphere as would be expected from the release pattern shown in Fig. 12. The above visual analysis might be taken further by subsequent analyses, but here is suffices to investigate if correlation analyses between the four DIFF12 atmospheric CO_2 records and the DIFF12 anthropogene CO_2 record support the result of the visual analysis.

Fig. 14 shows the calculated correlation coefficients between changes in anthropogene CO_2 and changes in atmospheric CO_2 for the four stations shown in Fig. 13. In all four cases there is a negative correlation from the time of release and 17–24 months later between DIFF12 changes in anthropogene CO_2 and DIFF12 changes in atmospheric CO_2,

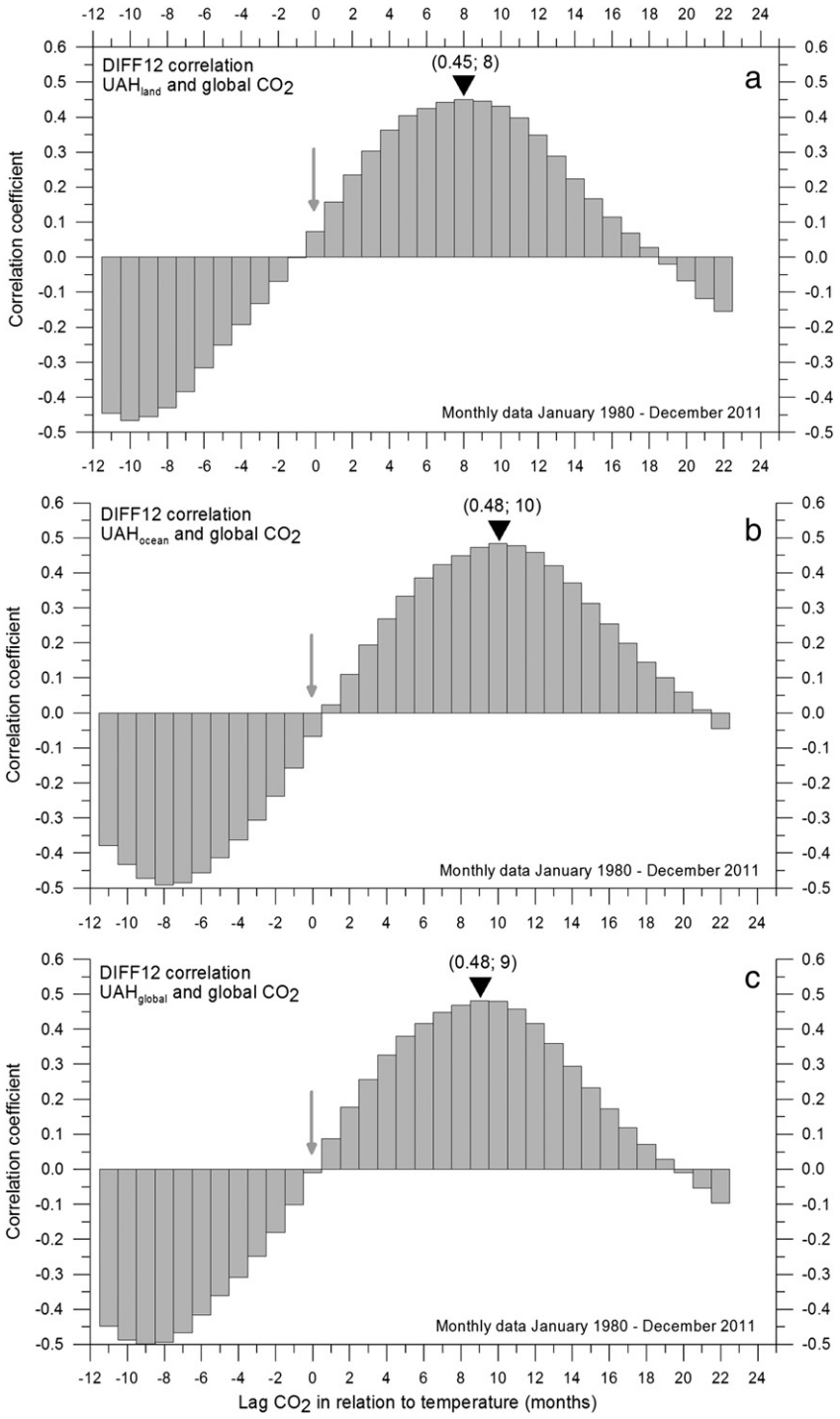

Fig. 8. Correlation coefficients between DIFF12 monthly lower troposphere temperatures (UAH) and global atmospheric CO_2, for different monthly lags of CO_2 in relation to temperature. The maximum positive correlation is found for CO_2 lagging 9 months after lower global troposphere temperatures, 10 months after lower troposphere temperatures over oceans, and 8 months after lower troposphere temperatures over land. Numbers in parentheses show the maximum positive correlation coefficient and the associated time lag of CO_2 in months. The grey vertical arrows indicate no lag.

showing that changes in the emission of anthropogene CO_2 are not causing changes in atmospheric CO_2. The strongest correlation coefficient ranges from −0.30 to −0.52, and the corresponding lag from 4 to 19 months, depending on latitude. The maximum absolute value of the negative correlation coefficient is larger for the Southern Hemisphere than for the Northern Hemisphere. On the other hand, the lag of DIFF12 for anthropogene CO_2 in relation to DIFF12 for atmospheric CO_2 is larger in the Northern Hemisphere than in the southern. Thus, there is no indication of a northern mid-latitude origin for DIFF12 changes in atmospheric CO_2. The lag is about 4 months for Ascension (8°S), 9 months for the South Pole (90°S), 14 months for Mauna Loa (20°N), and about 19 months for Alert (82°N) in the High Arctic. As each station is correlated with identical values (DIFF12 for anthropogene CO_2) the observed lags suggest a sequence of events starting near Equator in the Southern Hemisphere, and from there propagating towards the two poles.

Fig. 15 (panel a) shows the calculated correlation coefficient between changes in anthropogene CO_2 and changes in global

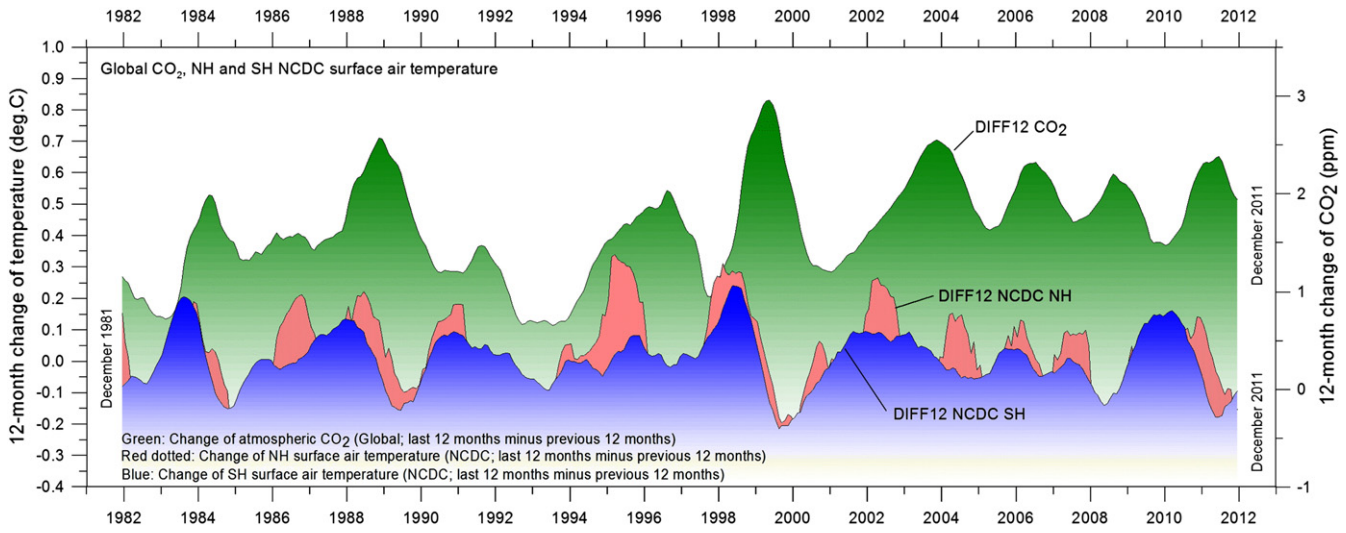

Fig. 9. 12-month change of global atmospheric CO_2 concentration (NOAA; green), change in Northern Hemisphere surface air temperature (NCDC; red dotted), and Southern Hemisphere air temperature (NCDC; blue). All graphs are showing monthly values of DIFF12, the difference between the average of the last 12 months and the average for the previous 12 months for each data series. (For interpretation of the references to color in this figure legend, the reader is referred to the web version of the article.)

atmospheric CO_2 for the entire period 1980–2011. It is seen that the correlation generally is low as was suggested by the visual analysis above, and noticeably smaller than found for correlations with temperatures (Figs. 4, 6, 8 and 10). From the time of release and to about 1 yr later there is a negative correlation between DIFF12 changes in anthropogene CO_2 and DIFF12 changes in atmospheric CO_2. The maximum positive correlation is found by correlating DIFF12 changes in CO_2 from fossil fuels with atmospheric CO_2

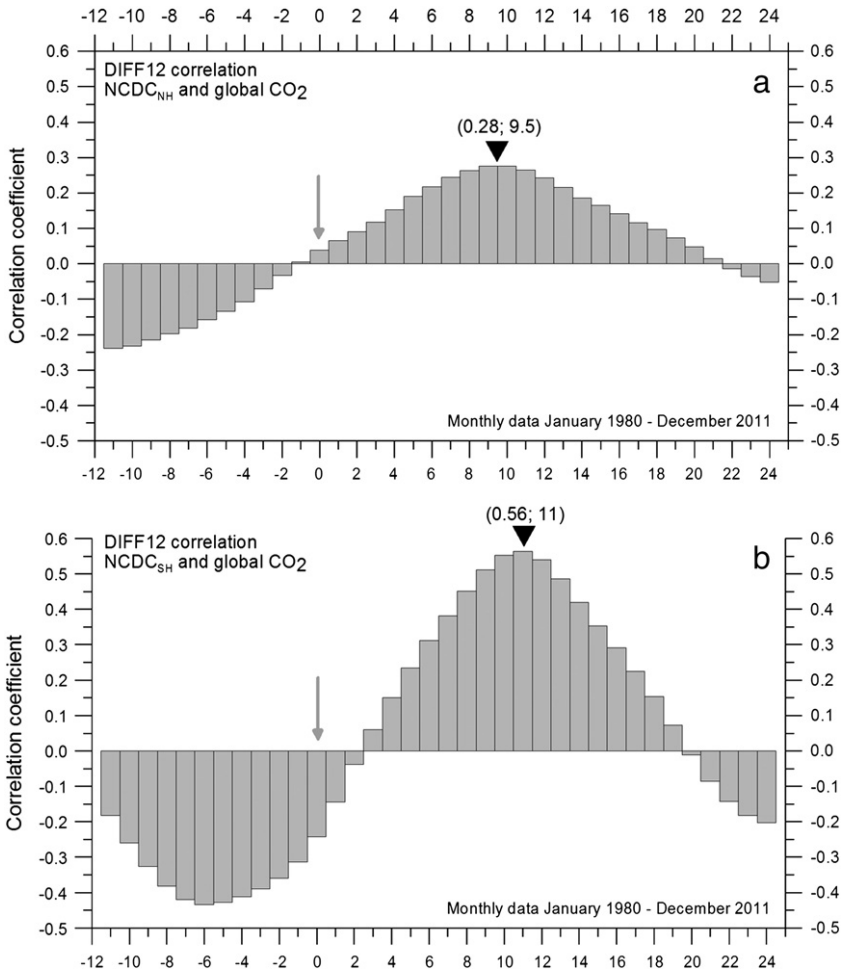

Fig. 10. Correlation coefficients between DIFF12 monthly surface air temperatures in the northern (a) and the Southern Hemisphere (b) and global atmospheric CO_2, for different monthly lags of CO_2. The maximum positive correlation is found for CO_2 lagging 9.5 months behind Northern Hemisphere temperature, and 11 months behind Southern Hemisphere temperature. Numbers in parentheses show the maximum positive correlation coefficient and the associated time lag of CO_2 in months. The grey vertical arrows indicate no lag.

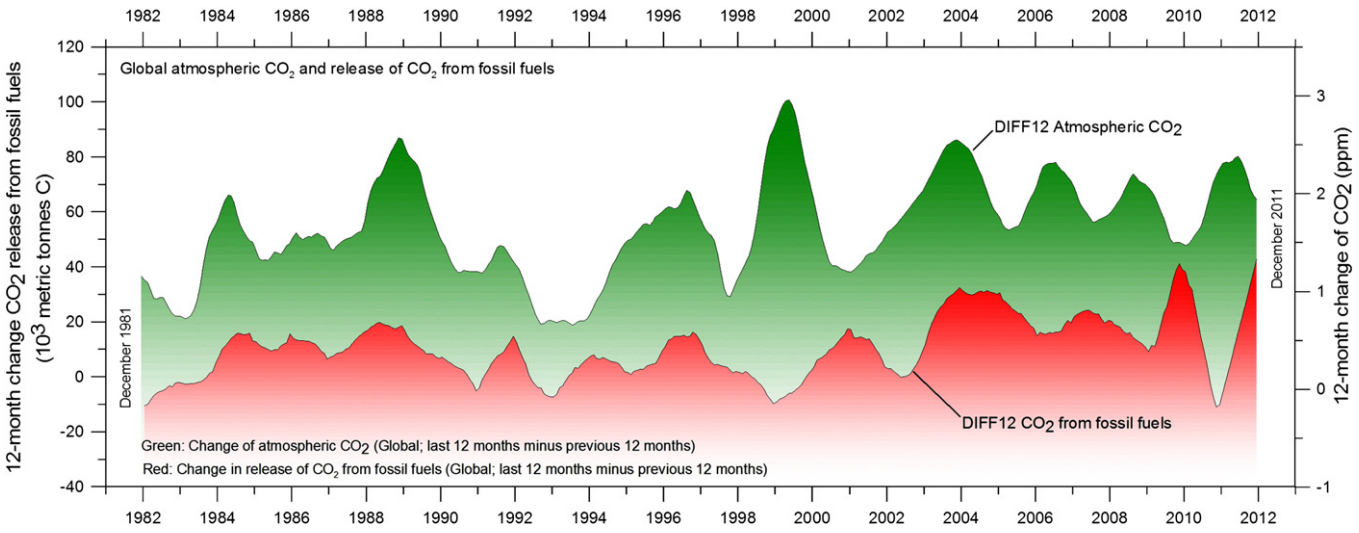

Fig. 11. 12-month change of global atmospheric CO_2 concentration (NOAA, green), and the change in release of CO_2 from burning of fossil fuels (CDIAC, red). Both graphs are showing monthly values of DIFF12, the difference between the average of the last 12 month and the average for the previous 12 months for each data series.

DIFF12 changes 11 months earlier. However, this is opposite to what would be expected if changes in anthropogene CO_2 had significant impact on changes in the amount of atmospheric CO_2.

However, on shorter time scales the relation is highly variable as the two panels b and c in Fig. 13 show. Dividing the entire observation period into the two sub-periods 1980–1998 and 1998–2011 yields a different result as to the correlation between DIFF12 changes in anthropogene CO_2 and DIFF12 changes in global atmospheric CO_2 (panel a). For the period 1980–1998 the correlation is found to be positive for the period at and following release, while it becomes negative for the time window 1998–2011. A positive correlation would indeed be expected, if changes in the release of anthropogene CO_2 were controlling changes in atmospheric CO_2. It is however contrary to expectation that the maximum positive correlation is found 1 month before the time of release (Fig. 15, panel b).

This demonstrates that the relation between changes in the release of CO_2 from anthropogene sources and changes in atmospheric CO_2 is not stable, but undergoes significant changes on a decadal time scale. Had changes in the release of anthropogene CO_2 represented the main control on changes in atmospheric CO_2, the relation would be stable. A possible explanation for the unstable correlation might be due to the combined El Niño–La Nino event 1997–2001, affecting the two investigated sub periods (Fig. 15) differently. Another possible explanation was provided by Njau (2007), suggesting that anthropogene CO_2 has so far been added to the atmosphere in an amount which would have otherwise been added naturally, especially by the warming oceans, had the emission of anthropogene CO_2 been absent. However, a detailed analysis of such and other possibilities falls beyond the present investigation, and here it suffices to conclude that the absence of a stable, positive correlation suggests other processes than the emission of anthropogene CO_2 to control the main features of the observed changes in atmospheric CO_2.

Summing up, our analysis suggests that changes in atmospheric CO_2 appear to occur largely independently of changes in anthropogene emissions. A similar conclusion was reached by Bacastow (1976), suggesting a coupling between atmospheric CO_2 and the Southern Oscillation. However, by this we have not demonstrated that CO_2 released by burning fossil fuels is without influence on the amount of atmospheric CO_2, but merely that the effect is small compared to the effect of other processes. Our previous analyses suggest that such other more important effects are related to temperature, and with ocean surface temperature near or south of the Equator pointing itself out as being of special importance for changes in the global amount of atmospheric CO_2.

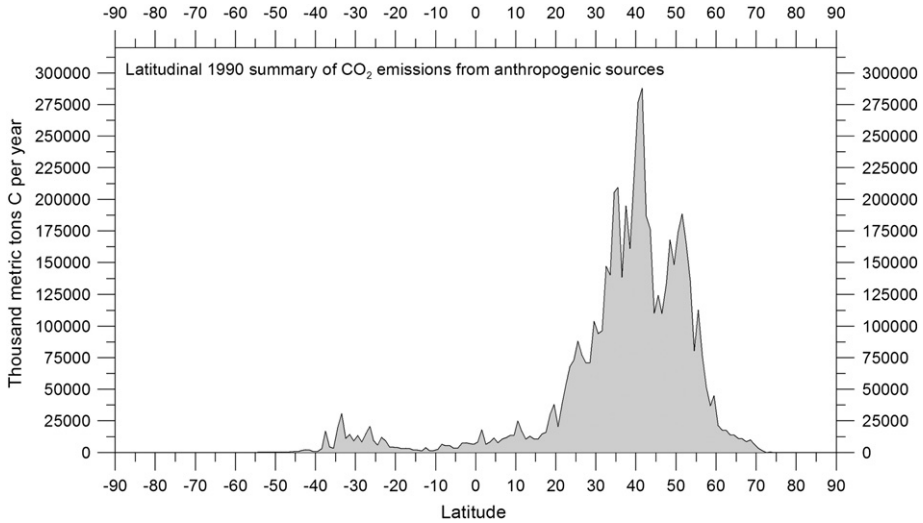

Fig. 12. Latitudinal 1990 summary of CO_2 emissions from anthropogene sources. Data source: Carbon Dioxide Information Analysis Center (CDIAC).

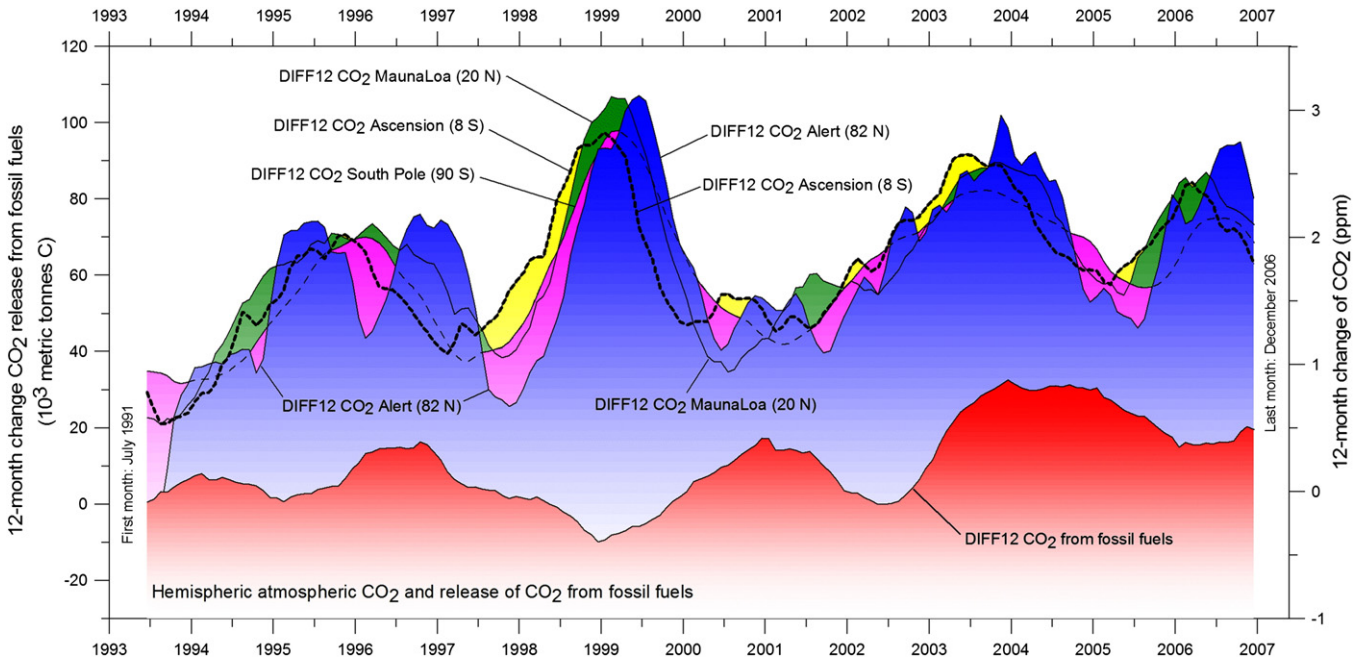

Fig. 13. 12-month change of global atmospheric CO_2 concentration for Alert (NOAA; blue), Mauna Loa (NOAA; green), Ascension Island (NOAA; yellow), and the south Pole (NOAA; purple), and the change in release of anthropogene CO_2 (CDIAC; red). All graphs show monthly values of DIFF12, the difference between the average of the last 12 months and the average for the previous 12 months for each data series. (For interpretation of the references to color in this figure legend, the reader is referred to the web version of the article.)

9. Volcanic eruptions

Volcanic eruptions are obviously relevant also to consider here, as they may contribute not only with tephra (e.g. ash), but also with substantial amounts of greenhouse gases such as H_2O and CO_2 to the atmosphere, influencing both temperature and the total amount of greenhouse gasses. In addition, a gas like SO_2 is injected into the atmosphere during eruptions. Oxidation and gas-to-particle conversion transforms SO_2 to sulphuric acid (H_2SO_4), which may effect cloud formation. Each year several volcanic eruptions occur globally, but the majority are small, and not significant within the present global context.

The reported magnitude of volcanic eruptions depends much on both the experience and vantage point of the observer. To meet the need for a meaningful magnitude measure that can be easily applied to eruption sizes, Newhall and Self (1982) therefore integrated quantitative data with the subjective descriptions of observers, resulting in the Volcanic Explosivity Index (VEI) to provide a relative measure of the explosiveness of volcanic eruptions. The VEI scale is a simple 0–8 index of increasing explosivity, based on volume of ejected mass, eruption cloud height, and other qualitative observations. The scale is logarithmic, with each interval on the scale representing a tenfold increase in observed ejecta criteria, with the exception of between VEI 0, VEI 1 and VEI 2. The VEI-divisions indicate the amount of tephra (volcanic ash) ejected into the atmosphere, but do not inform directly about the amount of water vapour and CO_2 emitted, but usually the amount of these is expected to follow roughly the VEI class, although with individual variations (see below). The most important characteristics of the individual VEI-classes are shown in Table 2.

Here we consider only eruptions greater than VEI size class 4, as these eruptions all are classified as large and therefore may have ejected significant of tephra and other eruption products to high altitudes, across the tropopause and into the stratosphere. The timing of such major volcanic eruptions since 1981 is shown in Fig. 16, together with the DIFF12 changes in the amount of atmospheric CO_2. Data on volcanic eruptions were obtained from the Global Volcanism Program (GWP).

As the VEI-data are qualitatively different from all previous data types used in the present analysis, being somewhat subjective and representing discrete events, we shun from attempting any kind of statistical analysis of these data, and will only consider briefly the visual impression gained from Fig. 16.

It is well known that major volcanic eruptions may influence global temperatures 4–5 yr (see, e.g., Lockwood and Fröhlich, 2008; Thompson et al., 2009) after the culmination of the eruption, although with variations reflecting the position of the volcano in relation to the Equator. The variable temperature effect of volcanic eruptions is illustrated by comparing the timing of major eruptions shown in Fig. 16 with the temperature graphs shown in Figs. 1, 2, 3, 5 and 7. For example, these diagrams all show global cooling after the very large Mount Pinatubo eruption that began in earnest June 1991. However, Fig. 16 shows that this very large eruption not to have resulted in any increase of atmospheric CO_2. The main DIFF12 change observed is actually a period of low growth rate for atmospheric CO_2. The same observation applies for the group of 2008 eruptions. This effect on CO_2 may be explained by volcanic gasses/aerosols and airborne debris affecting cloud cover, leading to cooling of the uppermost part of the oceans and therefore increased ability to take up atmospheric CO_2, according to Henry's law.

Summing up, although there has been several volcanic eruptions of at least VEI 4 during the study period, the direct effect on atmospheric CO_2 in general appears to be limited on the time scale investigated, and only contributes little to explain directly observed changes in atmospheric CO_2 within the study period. Perhaps eruptions larger than VEI = 6 are required to affect the global atmospheric composition and climate significantly, but there has been no eruptions of this magnitude during the study period. The analysis might be taken further by also considering the type of volcanism,

Fig. 14. Correlation coefficients between DIFF12 change in release of anthropogene CO_2 (CDIAC) and DIFF12 change in atmospheric CO_2 at different stations, for different lags of CO_2 in relation to CO_2 from fossil fuel. The maximum negative correlation is found for changes in atmospheric CO_2 ranges from 4 to 19 months after changes in CO_2 release from fossil fuels. Numbers in parentheses show the maximum absolute correlation coefficient and the associated time lag of CO_2 in months. The grey vertical arrows indicate no lag (the time of release).

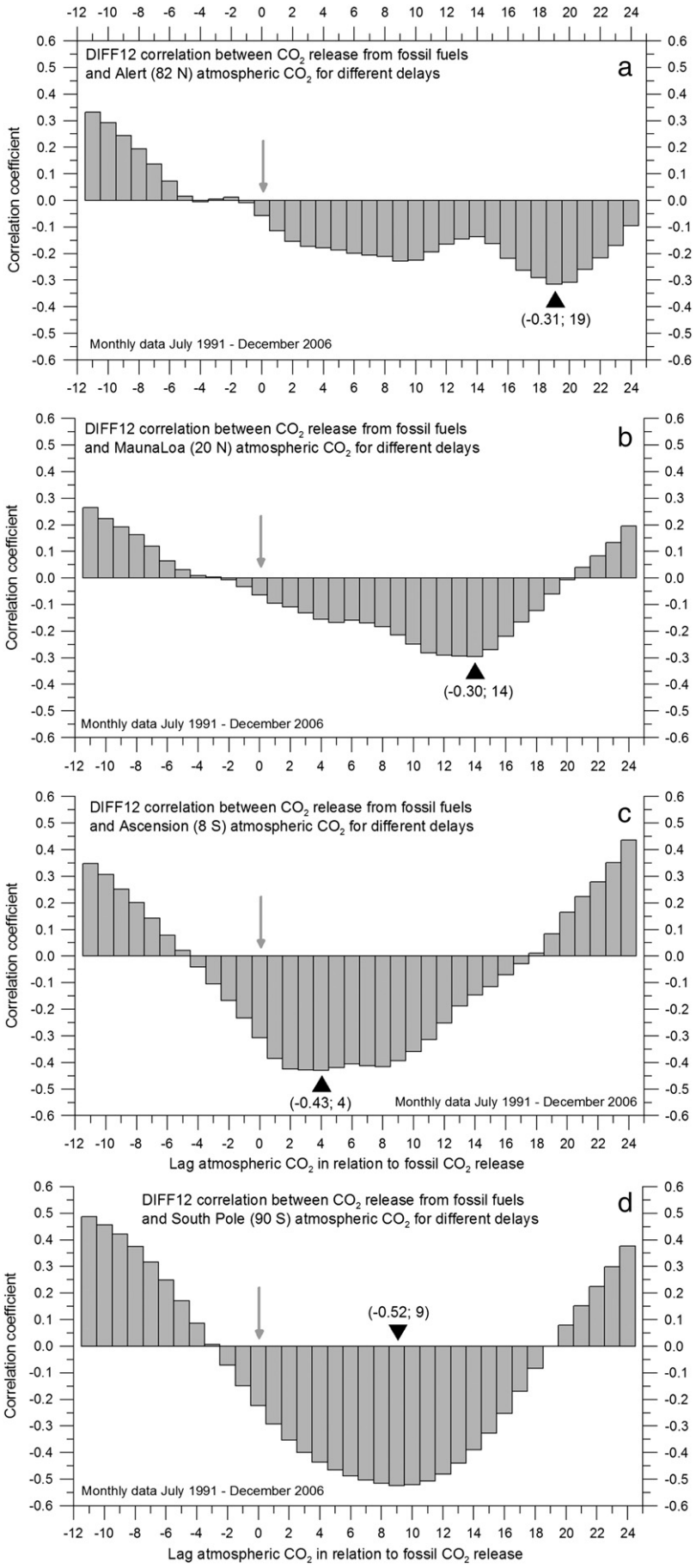

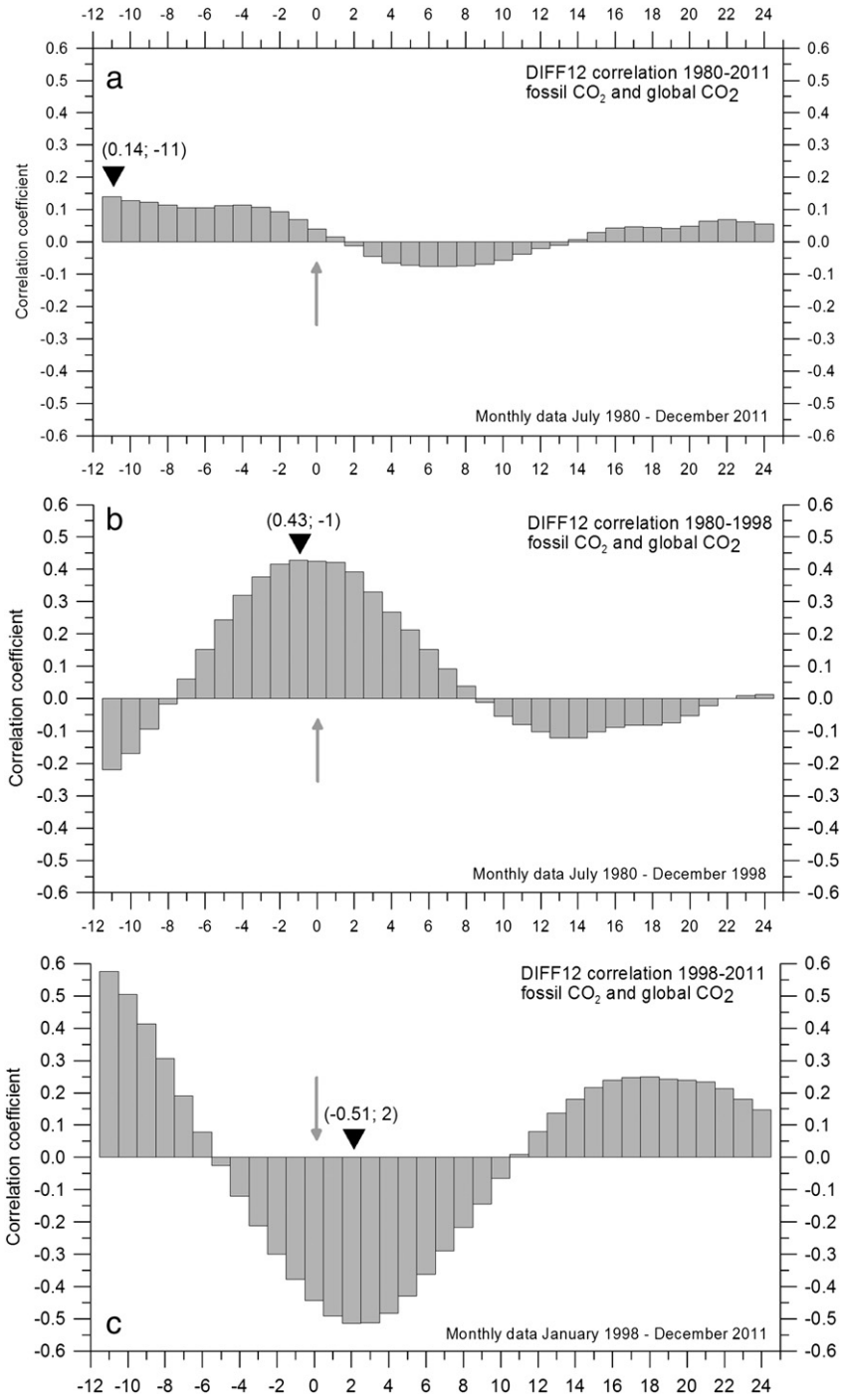

Fig. 15. Correlation coefficients between DIFF12 change in release of anthropogene CO_2 (CDIAC) and global atmospheric CO_2, for different lags of atmospheric CO_2 in relation to CO_2 from fossil fuel. Numbers in parentheses show the maximum positive correlation coefficient and the associated time lag of CO_2 in months. The grey vertical arrows indicate no lag (the time of release).

and from which depth in the crust it originates. In general, deep-seated volcanism is relatively rich in CO_2, while tholeiitic eruptions originating from more shallow depths usually are relatively rich in H_2O.

As was the case for anthropogene CO_2, we can therefore not conclude that volcanic activity since January 1980 is without influence on atmospheric CO_2, but only that the effect of eruptions in the study period apparently is small compared to other factors. On the time scale investigated here, the dominant effect of volcanic eruptions appears to be increased removal of CO_2 from the atmosphere by the oceans, presumably caused by volcanic eruptions affecting the global cloud cover, and thereby resulting in lower ocean surface temperature. On longer (geological) time scales the relation may however well be different.

10. Fourier frequency analyzes

Visual inspection of Figs. 2, 3, 5, 7 and 9 suggests that some DIFF12 series may be changing according to one or several rhythmic variations. Therefore, to investigate if these records are in fact characterized by such periodic variations, a Fourier frequency analysis was carried out on four key data series, 1) atmospheric CO_2 (NOAA), 2)

Table 2
Volcanic Explosivity Index (VEI) eruption size classes based on Newhall and Self (1982) and Simkin and Siebert (1994).

VEI class	0	1	2	3	4	5	6	7	8
Description	Non-explosive	Small	Moderate	Moderate–large	Large	Very large	Very large	Very large	Very large
Tephra (m^3)	$<1\times10^4$	$<1\times10^6$	$<1\times10^7$	$<1\times10^8$	$<1\times10^9$	$<1\times10^{10}$	$<1\times10^{11}$	$<1\times10^{12}$	$>1\times10^{12}$
Cloud height (km)	<0.1	0.1–1	1–5	3–15	10–25	>25	>25	>25	>25

HadCRUT3, 3) HadSST2 and 4) CO_2 released by use of fossil fuels (CDIAC). The results are shown in Fig. 17.

The DIFF12 atmospheric CO_2 record is seen to be dominated by two periods of about 3.8 and 2.5 yr length, both with amplitude greater than 0.25 ppm. The two DIFF12 temperature spectra are rather similar to each other, dominated by a period of about 3.7 yr length with amplitude greater than 0.09 °C, and both showing another important peak around 2.4 yr. The 2.5–2.4 yr period seen in the three uppermost records in Fig. 17 may possibly reflect the influence of the Southern Oscillation, as suggested by both Lamb (1972); Bacastow (1976). However, the spectrum for the DIFF12 CO_2 anthropogene record (lowermost panel in Fig. 13) is different. In particular, there is no frequency peak suggesting the existence of an important period in the range from 3.7 to 3.8 yr, which is a principal period length in the other three records, but the anthropogene CO_2 record does show a less pronounced peak around 4 yr. The potential implication of this peak will be commented later.

The significance levels shown in Fig. 17 are peak-based critical limit significance levels, which are of particular merit in ascertaining the significance of the largest spectral component (SeaSolve, 2003; Humlum et al., 2012). In this type of test, one seeks to disprove the null hypothesis postulating either a white noise signal with no autocorrelation (AR(1) = 0.0), or a red noise signal with autocorrelation (AR(1) > 0.0). Red noise is present when the background power decreases with increasing frequency, and the autoregressive value is a measure of the similarity between observations in a time series as a function of the time separation between them. All four DIFF12 series are characterized by high autocorrelation, with AR(1) coefficients ranging from 0.97 to 0.99.

With the background set, the peak spectral power was then compared against the various critical limits. A 99% critical limit is that level where in only 1 of 100 separate random noise signals the highest peak would achieve this height strictly due to random chance. Likewise, for a peak reaching the 50% critical limit there is a 50–50 probability that this could have arisen strictly from chance. The critical limit test used here is different from traditional confidence or significance levels that apply to a single data set only. For example, a standard 95% confidence limit would specify a level where 5% of the points in a single spectrum would be expected to lie above this height strictly due to random chance.

Exposed to the critical limit test all four DIFF12 series display several frequency peaks exceeding the 95% critical limit. For that reason the alternative null hypothesis, that the observed oscillations represent red noise only, can be rejected using a 95% peak-based critical limit test, and the significant frequency peaks are positively worthy of interpretation. Several peaks are seen to exceed even the 99% critical limit.

Comparing the different Fourier frequency spectra shown in Fig. 17, the degree of similarity between the two temperature records (HadCRUT3; HadSST2) and the atmospheric CO_2 record appears higher than the similarity between anthropogene CO_2 and atmospheric CO_2. This lends support to the result of the previous analyzes, that changes in atmospheric CO_2 appear to be coupled especially to changes in temperature, and not to the same degree to changes in CO_2 released by anthropogene sources.

The lower panel (d) in Fig. 17 indirectly shows the main rhythms of the world economy. However, the amount of anthropogene CO_2 must to some degree also reflect the production of heat and electricity for heating purposes, especially during winter in the Northern Hemisphere, as this is where most people live. Thus, it is not entirely surprising that the prominent temperature DIFF12 peak of about 3.7 yr (HadCRUT3 and HadSST2) may find itself represented in the broad frequency peak around 0.25 yr^{-1} (4 yr) in the DIFF12 data for anthropogene CO_2. The visual inspection of Fig. 11 leads to a similar interpretation.

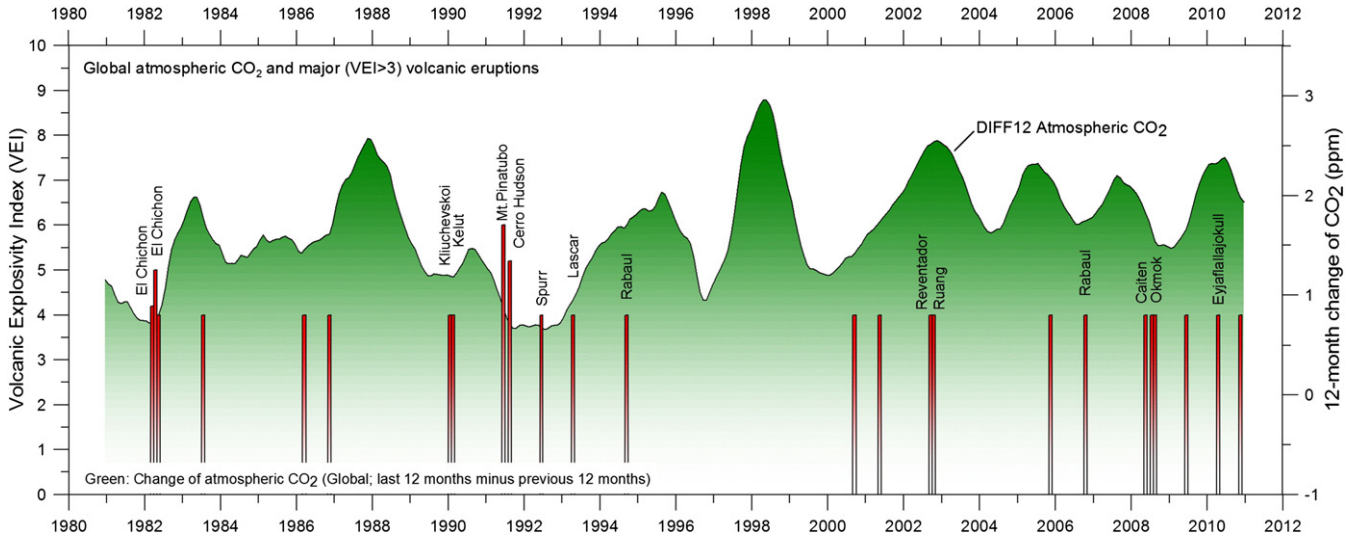

Fig. 16. 12-month change of global atmospheric CO_2 concentration (NOAA; green), and the timing of major (VEI > 3) volcanic eruptions (GWP). The CO_2 graph is showing monthly values of DIFF12, the difference between the average of the last 12 months and the average for the previous 12 months for each data series. The DIFF12 CO_2 values have been shifted 12 months forward to correspond correctly with the time axis used for plotting the volcanic eruptions.

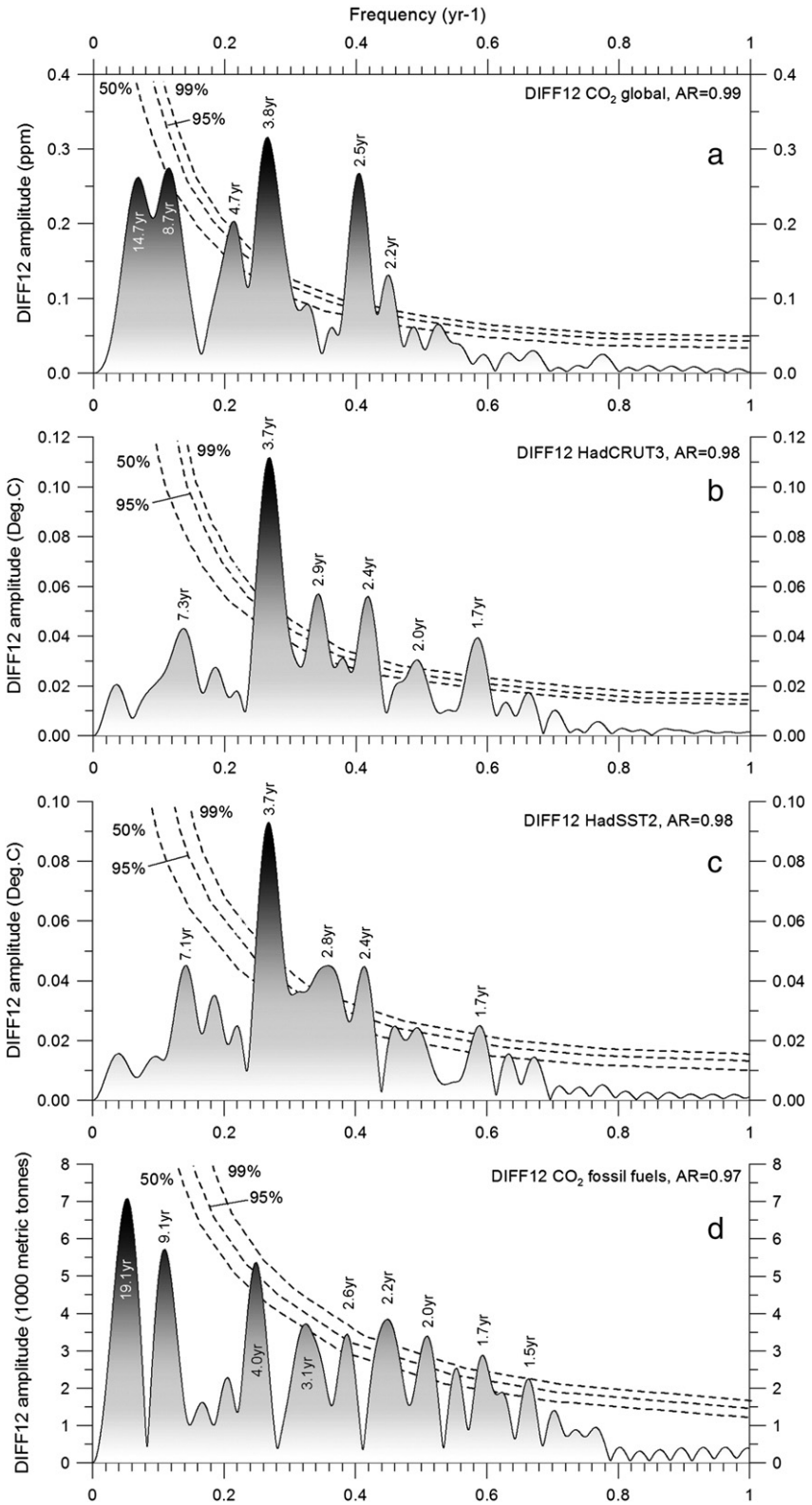

Fig. 17. Fourier frequency spectra (Best Exact N composite algorithm; SeaSolve, 2003) for DIFF12's for changes in a) atmospheric CO_2, b) HadCRUT3, c) HadSST2 and d) CO_2 released by use of fossil fuels. The DIFF12 atmospheric CO_2 record is dominated by highly significant periods of about 3.8 and 2.5 yr length, while especially a period of about 3.7 yr is dominant in both DIFF12 temperature records. The DIFF12 record for CO_2 from fossil fuels is characterized by a different type of spectrum, and with peaks of generally less significance than characterizing the other records. The grey tone indicates increasing amplitude within each record. The stippled lines indicate peak-based critical limit significance levels.

11. Discussion

By the above analysis we have demonstrated that there exists a clear phase relationship between the change of different global temperature indices, and corresponding changes in the global amount of atmospheric CO_2. We have used data on CO_2 and temperature with a monthly time resolution for the time window January 1980–December 2011, but instead of analyzing the monthly data,

we have removed the influence of annual cycles by analyzing DIFF12 values. The average DIFF12 CO_2 value for the entire observation period is about 1.7 ppm/yr, which adds up to the entire observed increase of 51 ppm of atmospheric CO_2 since January 1980. Therefore, to the degree that the observed DIFF12 atmospheric CO_2 values (Figs. 3, 5, 7 and 9) can be explained by temperature changes; the overall increase of atmospheric CO_2 since January 1980 (Fig. 1) is also explained.

The coupling from changes in atmospheric CO_2 to changes in temperature appears to be weak. The rate of temperature increase often decreases when the amount of atmospheric CO_2 increases (Figs. 2, 3, 5, 7 and 9). There are even several examples where the DIFF12 temperature change becomes negative (Table 1), corresponding to decreasing temperatures, even though the contemporary DIFF12 CO_2 change is positive.

In general, we find that changes in atmospheric CO_2 are lagging behind changes in any of the five different temperature records considered. The typical lag is 9.5–12 months for surface temperatures and about 9 months for lower troposphere temperatures, suggesting a temperature sequence of events from the surface to the lower troposphere.

As cause always must precede effect, this observation demonstrates that modern changes in temperatures are generally not induced by changes in atmospheric CO_2. Indeed, the sequence of events is seen to be the opposite: temperature changes are taking place before the corresponding CO_2 changes occur.

As the theoretical initial temperature effect of changes in atmospheric CO_2 must materialize first in the troposphere, and then subsequently at the planet surface (land and ocean), our diagrams 2–8 reveal that the common notion of globally dominant temperature controls exercised by atmospheric CO_2 is in need of reassessment. Empirical observations indicate that changes in temperature generally are driving changes in atmospheric CO_2, and not the other way around.

Numerical global climate models generally assume atmospheric CO_2 in combination with alleged feed-back effects on atmospheric humidity and cloud cover to have a clear net warming effect, and that changes in atmospheric CO_2 therefore represent a main driver for global temperature changes. For that reason changes in temperature should therefore be lagging behind corresponding changes in CO_2. However, Figs. 4, 6, 8 and 10 show correlation between changes in temperature and CO_2 to be negative for negative offsets (temperature lagging CO_2), indicating that changes towards higher concentrations of atmospheric CO_2 then empirically would associate with less rapid temperature increase or even a temperature decrease. However, as this would invalidate the basic assumption of CO_2 having a clear net warming effect, the perception of temperature lagging behind CO_2 must therefore be rejected. A visual inspection of the data displayed in Figs. 2, 3, 5, 7 and 9 also show the notion of temperature lagging CO_2 to be implausible.

Thus, the simplest explanation of observed changes in DIFF12 for atmospheric CO_2 is that they are induced by changes in temperature, as illustrated by Figs. 2–10. Consequently, a substantial part of the atmospheric increase of CO_2 since January 1980 can be explained by associated changes in temperature, and presumably especially changes in ocean temperatures (Toggweiler, 1999; Monnin et al., 2001; Goldberg, 2008), as this is where we find both the strongest correlation to changes in CO_2 (Figs. 4, 6 and 8), and the longest time lag.

The maximum positive correlation between ocean temperatures and atmospheric CO_2 is within a range from 0.45 to 0.48, depending on which dataset is considered (HadSST2, NCDC or UAH). With a sample size of 361 (number of monthly DIFF12 values) these correlation coefficients are highly significant at the 0.05 level, and correspond to a goodness-of-fit (r^2) ranging from 0.20 to 0.23. This represents a fair degree of explanation, and far bigger than achieved by any other factor considered in the present analysis, but it also suggests that there are other factors beyond ocean surface temperature which have influenced observed changes in atmospheric CO_2 since January 1980. Examples of such potential factors are changes in soil moisture, living biomass, volcanic eruptions, geological weathering processes, burning of fossil fuels, etc. The correlation between CO_2 released by anthropogene sources and changes in atmospheric CO_2 is not stable (Fig. 15), and not able to explain much of the observed increase in atmospheric CO_2 since January 1980. A qualitatively identical conclusion may possibly be suggested for the effect of volcanic eruptions during the study period, but the character of the volcanic data available does not make it possible to carry out a comparable statistical analysis on this. Actually, on the time scale investigated, the net effect of a major volcanic eruption appears to be a reduction of the prevailing increase rate of atmospheric CO_2, probably an effect of ocean cooling induced from cloud effects.

Summing up, monthly data since January 1980 on atmospheric CO_2 and sea and air temperatures unambiguously demonstrate the overall global temperature change sequence of events to be 1) ocean surface, 2) surface air, 3) lower troposphere, and with changes in atmospheric CO_2 always lagging behind changes in any of these different temperature records.

A main control on atmospheric CO_2 appears to be the ocean surface temperature, and it remains a possibility that a significant part of the overall increase of atmospheric CO_2 since at least 1958 (start of Mauna Loa observations) simply reflects the gradual warming of the oceans, as a result of the prolonged period of high solar activity since 1920 (Solanki et al., 2004). Based on the GISP2 ice core proxy record from Greenland it has previously been pointed out that the present period of warming since 1850 to a high degree may be explained by a natural c. 1100 yr periodic temperature variation (Humlum et al., 2011).

The atmospheric CO_2 growth rate DIFF12 is seen to be at maximum about the same time when SST DIFF12 is on the falling limb from a previous peak, indicating ocean temperature to be approaching a temperature maximum or falling after passing a peak (see, e.g., Fig. 2 and Table 1). As the rate of CO_2 net outgassing from the ocean then is affected by reduced solubility, this offers a simple physical explanation of the observed time lag. At least, the association between periods of maximum DIFF12 CO_2 increase and no or negative ocean surface temperature change (Table 1) is difficult to reconcile with the notion of atmospheric CO_2 changes controlling changes in ocean surface temperature. However, more work is needed to investigate the details of this, and it is worth noticing that atmospheric CO_2 increases over the period considered, even when air temperatures decreases. It is however clear from the data that emission of CO_2 from the oceans and other natural sources plays an important role in observed changes of atmospheric CO_2. Independent of human emissions, this contribution to atmospheric CO_2 is not controllable and little predictable, although the coupling to ocean surface temperature demonstrated above may provide a starting basis for future prediction attempts.

Analyses of a pole-to-pole transect of atmospheric CO_2 records suggest that changes in atmospheric CO_2 are initiated south of the Equator, but probably not far from the Equator, and from there spreads towards the two poles within a year or so (Fig. 13). This observation specifically points towards the oceans at or south of the Equator as an important source area for observed changes in atmospheric CO_2. The major release of anthropogene CO_2 is taking place at mid-latitudes in the Northern Hemisphere (Fig. 12), but the north–south transect investigated show no indication of the main change signal in atmospheric CO_2 originating here. The main signal must therefore be caused by something else. A similar conclusion, but based on studies of the residence time of anthropogenic CO_2 in the atmosphere, was reached by Segalstad (1998); Essenhigh (2009).

In general, the level of atmospheric CO_2 is slightly higher in the Northern Hemisphere than in the Southern Hemisphere. This might

be seen as due to anthropogene CO_2 mainly being released in the Northern Hemisphere (Fig. 12). However, had this being the explanation, the northern mid latitudes should had been the origin for changes in atmospheric CO_2, which is shown not to be the case (Figs. 13 and 14). Thus, presumably other processes are responsible for the north–south gradient in atmospheric CO_2, such as, e.g., respiration by land-based organisms (especially Northern Hemisphere) and ocean uptake (especially Southern Hemisphere).

Over the entire study period atmospheric CO_2 shows a continuous increase, when annual variations are ignored. This might also be interpreted as being the result of the release of anthropogene CO_2, but the observed propagation of the main atmospheric CO_2 change signal along the pole-to-pole transect (Fig. 13) seems to argue against such an interpretation. The signal propagation instead suggests a possible connection to especially the southern oceans and their surface temperature, but a detailed analysis of this falls beyond the present study.

The modern relation between temperature and CO_2 is qualitatively identical to that demonstrated by ice cores for the Quaternary glacial–interglacial transitions (Mudelsee, 2001; Caillon et al., 2003), although the modern time lag between temperature and CO_2 is considerably shorter. However, this is presumably reflecting the much coarser time resolution provided by ice cores, displaying only changes on a multi-decadal scale. This is partly due to sampling resolution, partly due to gas diffusion within the ice that averages out any surface temperature variability shorter than a few decades (Severinghaus et al., 1998).

12. Conclusions

There exist a clear phase relationship between changes of atmospheric CO_2 and the different global temperature records, whether representing sea surface temperature, surface air temperature, or lower troposphere temperature, with changes in the amount of atmospheric CO_2 always lagging behind corresponding changes in temperature.

(1) The overall global temperature change sequence of events appears to be from 1) the ocean surface to 2) the land surface to 3) the lower troposphere.
(2) Changes in global atmospheric CO_2 are lagging about 11–12 months behind changes in global sea surface temperature.
(3) Changes in global atmospheric CO_2 are lagging 9.5–10 months behind changes in global air surface temperature.
(4) Changes in global atmospheric CO_2 are lagging about 9 months behind changes in global lower troposphere temperature.
(5) Changes in ocean temperatures appear to explain a substantial part of the observed changes in atmospheric CO_2 since January 1980.
(6) CO_2 released from anthropogene sources apparently has little influence on the observed changes in atmospheric CO_2, and changes in atmospheric CO_2 are not tracking changes in human emissions.
(7) On the time scale investigated, the overriding effect of large volcanic eruptions appears to be a reduction of atmospheric CO_2, presumably due to the dominance of associated cooling effects from clouds associated with volcanic gases/aerosols and volcanic debris.
(8) Since at least 1980 changes in global temperature, and presumably especially southern ocean temperature, appear to represent a major control on changes in atmospheric CO_2.

Acknowledgments

The present study could not have been carried out without the existence of open-access international databases on temperature and atmospheric CO_2. We thank one unknown referee for pointing out the variable correlation between changes in the release of CO_2 from anthropogene sources and changes in atmospheric CO_2 on a decadal time scale. In addition, this referee suggested the hemispheric analyses (Section 7). We are finally grateful for informal discussions in Oslo with Drs. O.H. Ellestad, O. Engvold, and P. Brekke. Also Drs. T.V. Segalstad and H. Yndestad have for long time been important sources of information and inspiration.

References

Alley, R.B., Clarck, P.U., 1999. The deglaciation of the northern hemisphere: a global perspective. Annual Earth Planetary Science 27, 149–182.
Bacastow, R.B., 1976. Modulation of atmospheric carbon dioxide by the Southern Oscillation. Nature 261, 116–118.
Caillon, N., Severinghaus, J.P., Jouzel, J., Barnola, J.-M., Kang, J., Lipenkov, V.Y., 2003. Timing of atmospheric CO_2 and Antarctic temperature changes across Termination III. Science 299 (5613), 1728–1731.
Conway, T.J., Tans, P.P., Waterman, L.S., Thoning, K.W., Kitzis, D.R., Masarie, K.A., Zhang, N., 1994. Evidence for interannual variability of the carbon cycle from the NOAA/CMDL global air sampling network. Journal of Geophysical Research 99, 22831–22855.
Essenhigh, R.E., 2009. Potential dependence of global warming on the residence time (RT) in the atmosphere of anthropogenically sourced carbon dioxide. Energy & Fuels 23, 2773–2784.
Goldberg, F., 2008. Rate of increasing concentrations of atmospheric Carbon Dioxide controlled by natural temperature variations. Energy & Environment 19 (7), 67–77.
Humlum, O., Solheim, J.-E., Stordahl, K., 2011. Identifying natural contributions to late Holocene climate change. Global and Planetary Change 79, 145–156. http://dx.doi.org/10.1016/j.gloplacha.2011.09.005.
Humlum, O., Solheim, J.-E., Stordahl, K., 2012. Spectral analysis of the Svalbard temperature record 1912–2010. Advances in Meteorology 2012. http://dx.doi.org/10.1155/2012/175296 (Article ID 175296, 14 pages).
IPCC AR4, 2007. Contribution of Working Group I to the Fourth Assessment Report of the Intergovernmental Panel on Climate Change. Cambridge University Press, Cambridge, United Kingdom and New York, NY, USA.
Jaworowski, Z., Segalstad, T.V., Hisdal, V., 1992. Atmospheric CO_2 and Global Warming: A Critical Review, 2nd revised edition. : Letters, Vol. 119. Norwegian Polar Institute (76 pp.).
Keeling, C.D., Whorf, T.P., Wahlen, M., van der Plicht, J., 1995. Interannual extremes in the rate of rise of atmospheric carbon dioxide since 1980. Nature 375, 666–670.
Lamb, H.H., 1972. Climate: Present, Past and Future. : Fundamentals and Climate Now, Vol. 1. Methuen & Co Ltd., London (613 pp. SBN 416-11530-6).
Langenfelds, R.L., Francey, R.J., Pak, B.C., Steele, L.P., Lloyd, J., Trudinger, C.M., Allison, C.E., 2002. Interannual growth rate variations of atmospheric CO_2 and its delta C-13, H-2, CH4, and CO between 1992 and 1999 linked to biomass burning. Global Biogeochemical Cycles 16. http://dx.doi.org/10.1029/2001GB001466.
Lockwood, M., Fröhlich, C., 2008. Recent oppositely directed trends in solar climate forcings and the global mean surface air temperature. II. Different reconstructions of the total solar irradiance variation and dependence on response time scale. Proceedings of the Royal Society A 464, 1367–1385. http://dx.doi.org/10.1098/ispa.2007.0347.
Lorius, C., Raynaud, D., Jouzel, J., Hansen, J., Le Treut, H., 1990. The ice-core record—climate sensitivity and future greenhouse warming. Nature 347 (6289), 139–145.
Lüthi, D., Le Floch, M., Bereiter, B., Blunier, T., Barnola, J.-M., Siegenthaler, U., Raynaud, D., Jouzel, J., Fischer, H., Kawamura, K., Stocker, T.F., 2008. High-resolution carbon dioxide concentration record 650,000–800,000 years before present. Nature 453, 379–382. http://dx.doi.org/10.1038/nature06949.
Martin, P., Archer, D., Lea, D.W., 2005. Role of deep sea temperature in the carbon cycle during the last glacial. Paleoceanography 20 (2), 1–10.
Masarie, K.A., Tans, P.P., 1995. Extension and integration of atmospheric carbon dioxide data into a globally consistent measurement record. Journal of Geophysical Research 100, 11593–11610.
Monnin, E., Indermühle, A., Dällenbach, A., Flückiger, J., Stauffer, B., Stocker, T.F., Raynaud, D., Barnola, J.-M., 2001. Atmospheric CO_2 concentrations over the last glacial termination. Science 291, 112–114.
Mudelsee, M., 2001. The phase relations among atmospheric CO_2 content, temperature and global ice volume over the past 420 ka. Quaternary Science Reviews 20, 583–589.
Nakazawa, T., Moromoto, S., Aoki, S., Tanaka, M., 1997. Temporal and spatial variations of the carbon isotopic ratio of atmospheric carbon dioxide in the Western Pacific region. Journal of Geophysical Research 102, 1271–1285.
Newhall, C.G., Self, S., 1982. The volcanic explosivity index (VEI): an estimate of explosive magnitude for historical volcanism. Journal of Geophysical Research-Oceans & Atmospheres 87, 1231–1238.
Njau, E.C., 2007. Formulations of human-induced variations in global temperature. International Journal of Renewable Energy 32, 2211–2222.
Scafetta, N., 2011. Testing an astronomically based decadal-scale empirical harmonic climate model versus the IPCC (2007) general circulation climate models. Journal of Atmospheric and Solar-Terrestrial Physics. http://dx.doi.org/10.1016/j.jastp.2011.12.005.
SeaSolve, 2003. AutoSignal. Pioneering Automated Signal Analysis and Advanced Filtering. User's Manual. SeaSolve Software Inc., Framingham, MA, USA.
Segalstad, T.V., 1998. Carbon Cycle Modelling and the Residence Time of Natural and Anthropogenic Atmospheric CO_2: On the Construction of the "Greenhouse Effect

Global Warming" Dogma. In: Bate, R. (Ed.), Global Warming: The Continuing Debate. ESEF, Cambridge, U.K. ISBN: 0952773422, pp. 184–219.
Severinghaus, J.P., Sowers, T., Brook, E.J., Alley, R.B., Bender, M.L., 1998. Timing of abrupt climate change at the end of the Younger Dryas interval from thermally fractionated gases in polar ice. Nature 391, 141–146. http://dx.doi.org/10.1038/34346.
Shackleton, N.J., 2000. The 100,000 year ice-age cycle identified and found to lag temperature, carbon dioxide and orbital eccentricity. Science 289, 1897–1902.
Shakun, J.D., Clark, P.U., He, F., Marcott, S.A., Mix, A.C., Liu, Z., Otto-Bliesner, B., Schmittner, A., Bard, E., 2012. Global warming preceded by increasing carbon dioxide concentrations during the last deglaciation. Nature 484, 49–55. http://dx.doi.org/10.1038/nature10915.
Simkin, T., Siebert, L., 1994. Volcanoes of the World, 2nd edition. Geoscience Press in association with the Smithsonian Institution Global Volcanism Program, Tucson AZ . (368 pp.).
Solanki, S.K., Usoskin, I.G., Kromer, B., Schüssler, M., Beer, J., 2004. Unusual activity of the Sun during recent decades compared to the previous 11,000 years. Nature 431, 1084–1087.
Stauning, P., 2011. Solar activity–climate relations: a different approach. Journal of Atmospheric and Solar-Terrestrial Physics 73, 1999–2012.
Thompson, D.W.T., Wallace, J.M., Jones, P.D., Kennedy, J.J., 2009. Identifying signatures of natural climate variability in time series of global-mean surface temperature. Methodology and insights. Journal of Climate 22, 6120–6141. http://dx.doi.org/10.1175/2009JCLI3089.1.
Toggweiler, J.R., 1999. Variation of atmospheric CO_2 by ventilation of the ocean's deepest water. Paleoceanography 14 (5), 571–588.
Toggweiler, J.R., Lea, D.W., 2010. Temperature differences between the hemispheres and ice age climate variability. Palaeoceanography 25, PA2212.

Web references

CO_2 globally averaged marine surface data (accessed March 11, 2012): ftp://ftp.cmdl.noaa.gov/ccg/co2/trends/co2_mm_gl.txt
HadCRUT3 monthly global surface air temperature (accessed March 11, 2012): http://www.metoffice.gov.uk/hadobs/hadcrut3/diagnostics/global/nh+sh/monthly
HadSST2 monthly global sea surface temperature (accessed March 11, 2012): http://www.cru.uea.ac.uk/cru/data/temperature/hadsst2gl.txt
UAH monthly global lower troposphere temperature (accessed March 11, 2012): http://vortex.nsstc.uah.edu/data/msu/t2lt/uahncdc.lt
Goddard Institute for Space Studies, GISS (accessed March 11, 2012): http://data.giss.nasa.gov/gistemp/tabledata_v3/GLB.Ts+dSST.txt
National Climatic Data Center, NCDC (accessed March 11, 2012): http://www.ncdc.noaa.gov/cmb-faq/anomalies.phpIndividual station atmospheric CO_2 records from
Earth System Research Laboratory, NOAA (accessed July 25, 2012): http://www.esrl.noaa.gov/gmd/ccgg/iadv/
Carbon Dioxide Information Analysis Center, CDIAC (accessed March 11, 2012): http://cdiac.ornl.gov/epubs/fossil_fuel_CO2_emissions_gridded_monthly_v2011.html
Global Volcanism Program, GWP (accessed March 11, 2012): http://www.volcano.si.edu/world/largeeruptions.cfm